People's Democratic Republic of Algeria

Ministry of Higher Education and Scientific Research

Echahid Cheikh Larbi Tebessi University- Tébessa

Faculty of Exact Sciences and Natural and Life Sciences

Department of Computer Science

Master's Thesis For obtaining the

MASTER diploma

***Domain** : Mathematics and Computer Science*

***Field** : Computer Science*

***Specialty:** Systems and Multimedia*

Title

Animal Skin Disease Identification Using Machine Learning Methods

***Presented by:** Serradj Zahia*

In Front Of The Jury :

Mr. **Lakhdar LAIMECHE**	*Professor*	*Univérsité Echahid Cheikh Larbi Tébessi*	***President***
Mr. **Fathi HAMIDANE**	*Assistant Professor (A)*	*Univérsité Echahid Cheikh Larbi Tébessi*	***Examiner***
Mr. **Abdeljalil GATTAL**	*Professor*	*Univérsité Echahid Cheikh Larbi Tébessi*	***Supervisor***
Mr. **Yahya MENASSEL**	*Associate Professor (B)*	*Univérsité Echahid Cheikh Larbi Tébessi*	***Co- Supervisor***

***University Year :** 2024/2025*

Acknowledgment

I would like to begin by thanking Allah for granting me the strength, patience, and perseverance to complete this work.

I extend my sincere gratitude to:

*My supervisor**, Mr. Abdeljalil GATTAL ,** for his invaluable guidance, continuous support, and encouragement throughout the course of this project. His advice and insightful remarks were of great help and played a key role in the completion of this research.*

I would also like to express my deep appreciation to my co-supervisor,
***Mr. Yahia MENASSEL ,** for his assistance, constructive feedback, and the time he devoted to helping me overcome the challenges I encountered.*

*My sincere thanks go as well to the members of the jury, **Mr. Lakhdar LAIMECH** and **Dr. Fathi HMIDANE ,** for accepting to evaluate this work and for their valuable comments.*

I also wish to thank all the professors who contributed to my academic journey and shared their knowledge and experience during my studies.

My appreciation goes to my colleagues and everyone who supported me in any way during this journey.

Finally, I express my heartfelt thanks to my family for their constant encouragement, love, and support throughout my academic path.

Thank you all.

شكر و عرفان

الحمد لله حبًا وشكرًا وامتنانًا على البدء والختام، وآخر دعوانا أن الحمد لله رب العالمين.

بكل حب وامتنان، أهدي ثمرة جهدي وتخرجي...

إلى من زيّن اسمي بأجمل الالقاب، من منحني الدعم بلا حدود، والعطاء بلا مقابل، سندي الاول في مسيرتي، وملاذي بعد الله، فخري واعتزازي، والدي الذواديّ، أطال الله في عمره وأدامه لي عزًا وسندًا.

إلى من جعل الله الجنة تحت أقدامها، من احتضنني قلبها قبل يديها، وكانت دعواتها لي ضوءًا في عتمة الطريق، أمي نصيرة، يا سر قوتي ونبع حناني، يا شمعة أيامي، وجنتي في دنياي.

إلى السند الذي لا يميل، ورفيقي في درب الحياة، إلى من كانت كلماته عزاءً وقلبه وطنًا، أخي محمد، دمت لي قوة وأمانًا مدى الدهر.

إلى الضلع الثابت وأمان أيامي...

إلى من كنّ لي عونًا وسندًا، وكنزًا لا يُعوّض، إلى صفوة الأيام ونبض القلب، أخواتي الغاليات: صفاء، خولة، ملاك، ورحمة.

إلى قرة عيني وزينة أيامي، أبناء وبنات أخواتي الأعزاء: أريج، فراس، إسلام، وسيم، أنتم البهجة التي تملأ قلبي، والدافع الذي يزيدني إصرارًا.

إلى كل من أحبهم ويعرفني، لكم من القلب كل الحب والتقدير.

أهديكم هذا الإنجاز الذي لطالما حلمت به، فالحمد لله الذي وهبني إياه، وأسأله أن يعينني ويجعلني مباركة أينما كنت.

وأخيرًا، من قال "أنا لها" نالها... وأنا لها، وإن أبت، جئت بها رغمًا عنها.

تذكّر دائمًا: أن الحياة تتطلب شجاعة لنكون نحن، شجاعة لنحلم، وشجاعة أعظم لنحوّل تلك الأحلام إلى واقع... فكن فخورًا بما وصلت إليه.



Abstract

Skin diseases in animals are a growing concern in veterinary medicine, particularly in rural and underserved areas that lack access to specialized care services. With the rapid advancements in computer vision and artificial intelligence techniques, novel methods have emerged to facilitate the early and accurate diagnosis of these pathological conditions.

This research proposes a predictive approach based on deep learning techniques, utilizing Convolutional Neural Networks (CNNs) and multispectral imaging to detect and classify skin diseases in dogs. The work is divided into three main axes: the first axis covers the fundamentals of animal skin diseases, their clinical importance, and traditional diagnostic methods. The second axis discusses the role of Transfer Learning and the use of state-of-the-art neural network architectures in medical image classification. The third axis details the experimental protocol, which includes the use of multispectral images, the class_weight technique to address data imbalance, and the evaluation of several CNN models such as **Xception**, **EfficientNet**, and **DenseNet121**.

The results demonstrated that the **Xception** model outperformed the other models, achieving an accuracy of **98.9%**, an Area Under the Curve (AUC) of **99.7%**, and a Matthews Correlation Coefficient (MCC) of **98.4%**. These findings highlight the efficacy of combining multispectral imaging with deep learning techniques in veterinary diagnostics and underscore the significant potential of AI-powere d tools in enhancing animal health, especially in resource-limited regions.

الملخص

تُعد الأمراض الجلدية لدى الحيوانات مصدر قلق متزايد في مجال الطب البيطري، لا سيما في المناطق الريفية والمحرومة التي تفتقر إلى خدمات الرعاية المتخصصة. ومع التقدم السريع في تقنيات الرؤية الحاسوبية والذكاء الاصطناعي، ظهرت طرق جديدة تهدف إلى تسهيل التشخيص المبكر والدقيق لهذه الحالات المرضية.

يقترح هذا البحث مقاربة تنبؤية تعتمد على تقنيات التعلم العميق، وذلك باستخدام الشبكات العصبية الالتفافية (CNN) والتصوير متعدد الأطياف لاكتشاف وتصنيف الأمراض الجلدية لدى الكلاب. ينقسم العمل إلى ثلاثة محاور رئيسية: يتناول المحور الأول أساسيات الأمراض الجلدية الحيوانية وأهميتها السريرية وطرق التشخيص التقليدية، بينما يعرض المحور الثاني دور التعلم بالنقل (Transfer Learning) واستخدام أحدث معماريات الشبكات العصبية في تصنيف الصور الطبية، أما المحور الثالث فيُفصّل البروتوكول التجريبي الذي يتضمن استخدام الصور متعددة الأطياف، وتقنية وزن الفئات (class_weight) لمعالجة عدم توازن البيانات، بالإضافة إلى تقييم عدة نماذج CNN مثل Xception وEfficientNet وDenseNet121.

أظهرت النتائج أن نموذج Xception تفوق على النماذج الأخرى، حيث حقق دقة بلغت **98.9%**، ومنحنى AUC بنسبة **99.7%**، ومعامل ارتباط ماثيوز (MCC) بنسبة **98.4%**. تُبرز هذه النتائج فعالية الجمع بين التصوير متعدد الأطياف وتقنيات التعلم العميق في التشخيص البيطري، وتؤكد على الإمكانات الكبيرة للأدوات المدعومة بالذكاء الاصطناعي في تعزيز صحة الحيوانات، خاصة في المناطق ذات الموارد المحدودة.

Résumé

Les maladies cutanées chez les animaux représentent une préoccupation croissante en médecine vétérinaire, en particulier dans les régions rurales et mal desservies, où l'accès aux soins spécialisés est limité. Avec les avancées de la vision par ordinateur et de l'intelligence artificielle, de nouvelles méthodes ont émergé pour faciliter le diagnostic précoce et précis de ces affections.

Cette étude propose une approche prédictive basée sur l'apprentissage profond, en exploitant spécifiquement les réseaux de neurones convolutifs (CNN) et l'imagerie multispectrale pour détecter et classer les maladies de la peau chez les chiens. Le travail est structuré en trois parties principales : la première explore les fondements des maladies cutanées animales, leur importance clinique et les méthodes de diagnostic existantes ; la deuxième présente les apports de l'apprentissage par transfert et des architectures CNN modernes dans la classification d'images médicales ; enfin, la troisième partie détaille le protocole expérimental, incluant l'utilisation d'images multispectrales, l'application de la pondération des classes (class_weight) pour gérer le déséquilibre des données, et l'évaluation de plusieurs modèles CNN tels que Xception, EfficientNet et DenseNet121.

Les résultats révèlent que le modèle Xception surpasse les autres, atteignant une précision de 98,9 %, une AUC de 99,7% et un coefficient de corrélation de Matthews de 98,4% . Ces résultats démontrent l'efficacité de la combinaison entre imagerie multispectrale et apprentissage profond pour le diagnostic vétérinaire, et soulignent le potentiel des outils assistés par l'IA pour améliorer la santé animal

Table of Contents

Abstract i
الملخص ii
Résumé iii
Table of Contents iv
List Of Figures vii
List Of Tables viii
List of Abbreviations ix

General Introduction

General Introduction 2

Chapter 1 : Skin Diseases

1. Introduction: 4
2. Structure and Function of the Skin 4
   2.1. Structure of the Skin 4
      2.1.1 The Epidermis 5
      2.1.2 The Dermis 6
      2.1.3 The Hypodermis 7
   2.2 Functions of the Skin 8
      2.2.1 Protective Function 8
      2.2.2 Thermoregulation 8
      2.2.3 Sensory Perception 8
      2.2.4 Excretion and Secretion 9
      2.2.5 Immune Defense 9
      2.2.6 Vitamin D Synthesis 9
3. Overview of Skin Diseases 9
   3.1 Skin Diseases in Humans 9
      3.1.1 Infectious Diseases 9
      3.1.2 Inflammatory and Autoimmune Diseases 10
      3.1.3 Allergic and Environmental Diseases 11
   3.2 Skin Diseases in Animals 11
      3.2.1 Infectious Diseases 11
      3.2.2 Autoimmune and Allergic Diseases 11

3.2.3 Hormonal and Metabolic Diseases 12
4. Current Challenges in Diagnosing Skin Diseases 12
5. Background and Problem Statement 12
5.1 Machine Learning 13
5.2 Deep Learning 13
5.3 Hybrid Approaches 13
6. Conclusion 14

Chapter 2 : Rlated Work

1. Introduction 16
2. Related Work 16
2.1. Classical Machine Learning-Based Approaches 16
2.2. Deep Learning (DL)-Based Approaches 18
2.3. Hybrid Approaches 20
3. Main Datasets 22
4. Comparative Summary 26
5. Conclusion 28

Chapter 3 : Experimental Evaluation and Results

1. Introduction 30
2.1. Python 30
2.2. Kaggle 31
2.3. NumPy 31
2.4. Matplotlib 31
2.5. Scikit-learn 32
2.6. TensorFlow 32
2.7. Keras 32
2.8. Jupyter Notebook 33
3. Description of the Dataset Used 33
4. Data Preprocessing and Dataset Splitting 34
5. Models Selection 35
5.1. Transfer Learning 35
5.2. Evaluated Pre-trained Models 35
5.2.1 Architectural Families of Pre-trained Models 36
➤ ResNet (Residual Networks) 36

➤ DenseNet (Densely Connected Convolutional Networks) 37
➤ Xception (Extreme Inception) 39
➤ EfficientNet 39
➤ MobileNet Family 41
5.3. Selected Models 42
5.4. Training Strategy of the Selected Pre-trained Models 43
5.4.1 Training Parameters 44
5.4.2 Training and Evaluation Protocol 44
6. Evaluation Results 44
6.1. Evaluation Metrics 44
6.2 Performance of CNN Models on original Multispectral Images 46
6.3. Performance of the Xception Model Using Data Augmentation 48
6.3.1 Performance Comparison Before and After Applying Data Augmentation 50
7. Comparative Analyses 52
8. Limitations and Future Perspectives 53
8.1. Limitations 53
8.2. Future Perspectives 53
7. Conclusion 54

General Conclusion

General Conclusion 56
Bibliography 57

List Of Figures

Figure 1: Diagram of the three main layers of the skin 5
Figure 2: Structure of the epidermis 6
Figure 3: Structure of the Dermis 7
Figure 4:Structure of the hypodermis 7
Figure 5: Python Logo 30
Figure 6: Kaggle Logo 31
Figure 7: Numpy Logo 31
Figure 8: Matplotlib Logo 31
Figure 9: Scikit-Learn Logo 32
Figure 10: TensorFlow Logo 32
Figure 11: Keras Logo 33
Figure 12: Residual connections. 36
Figure 13: Example of an Inception model 37
Figure 14: Example of an InceptionV3 model 37
Figure 15: Architecture of DenseNet 38
Figure 16: DenseNet-121 architecture 38
Figure 17: Xception (Extreme Inception) architecture 39
Figure 18: EfficientNet architecture 40
Figure 19: Architecture of EfficientNet-B0 40
Figure 20: Architecture of EfficientNet-B3 41
Figure 21 : Architecture of EfficientNet-B7 41
Figure 22: MobileNetV2 Architecture 42
Figure 23: Bar chart comparing the performance of various CNN models on multispectral images in terms of Accuracy, F1-score, and AUC. 48
Figure 24: Training and validation accuracy and loss curves of the Xception model after applying data augmentation. 49
Figure 25: Confusion Matrices of the Xception Model Before and After Data Augmentation. 50
Figure 26: Performance Comparison of the Xception Model With and Without Data Augmentation. 51

List Of Tables

Table 1 . Summary of Related Works on Skin Disease Detection 27
Table 2 . Overview of Classes in the Multispectral Image Dataset 34
Table 3 . Dataset Splitting and Preparation for Training 35
Table 4 . Performance of different CNN models on multispectral images**.** 46
Table 5 . Comparative Performance of the Xception Model with and without Data Augmentation... 50
Table 6 . Comparative summary of methodologies and results..... 52

List of Abbreviations

- **AI**: Artificial Intelligence
- **ML**: Machine Learning
- **DL**: Deep Learning
- **UV**: Ultraviolet
- **HSV**: Herpes Simplex Virus
- **HPV**: Human Papillomaviruses
- **SVM**: Support Vector Machines
- **k-NN**: k-Nearest Neighbors
- **CNN**: Convolutional Neural Networks
- **FAD**: Flea Allergy Dermatitis
- **LSD:** Lumpy Skin Disease
- **RF:** Random Forest
- **Poly-F:** Polynomial Features
- **DT:** Decision Tree
- **MAE:** Mean Absolute Error
- **MSE:** Mean Squared Error
- **RMSE:** Root Mean Squared Error
- **ANN:** Artificial Neural Network
- **ReLU:** Rectified Linear Unit
- **ECA:** Efficient Channel Attention
- **GCT:** Global Context Transformer
- **AUC:** Area Under the Curve
- **GAN:** Generative Adversarial Network
- **CBAM:** Convolutional Block Attention Module
- **DCGAN:** Deep Convolutional Generative Adversarial Network
- **MCC:** Matthews Correlation Coefficient
- **VGG:** Visual Geometry Group
- **ISIC:** International Skin Imaging Collaboration
- **HAM10000:** Human Against Machine with 10,000 training images
- **LBP:** Local Binary Pattern
- **LSTM:** Long Short-Term Memory
- **DermIS:** Dermatology Information System
- **FCN:** Fully Convolutional Networks
- **XML:** Extensible Markup Language
- **JSON:** JavaScript Object Notation
- **GPU:** Graphics Processing Unit
- **ROC:** Receiver Operating Characteristic

General Introduction

General Introduction

Skin diseases in animals, especially in dogs, are a common veterinary issue that can reflect broader health problems. However, access to specialized diagnostic expertise remains limited in many rural and underserved areas. In this context, the integration of Artificial Intelligence (AI), particularly deep learning, offers promising solutions for developing accessible and reliable diagnostic tools.

Recent advances in computer vision have enabled the use of Convolutional Neural Networks (CNNs) for accurate image classification in medical and veterinary fields. Additionally, multispectral imaging has improved the detection of subtle skin abnormalities beyond the capabilities of standard RGB imaging.

This study aims to develop a predictive model for classifying canine skin diseases using transfer learning and multispectral data. Various advanced CNN architectures—such as Xception, EfficientNet, and DenseNet ……etc were employed, and class imbalance was addressed using the class_weight method. Model evaluation was conducted using Accuracy, AUC, MCC, and F1-score.

The structure of this work is organized into three main chapters: the first chapter presents a general overview of skin diseases in animals and their significance; the second chapter explores the contribution of artificial intelligence and deep learning in veterinary applications; finally, the third chapter describes the proposed model, the technical implementation steps, and a detailed analysis of the experimental results.

Chapter 1 : Skin Diseases

1. Introduction:

Diseases affect both humans and animals, posing significant threats to health and quality of life. In animals, such conditions can reduce agricultural productivity, endanger the health of domestic species, and contribute to the spread of zoonotic diseases. Therefore, early and accurate diagnosis is essential to improve treatment outcomes and limit transmission.

Recent advances in artificial intelligence (AI), particularly in machine learning (ML) and deep learning (DL), have enabled the development of automated systems for detecting and classifying skin diseases from visual data. These technologies offer fast and reliable analysis, potentially reducing dependence on veterinary specialists—especially in underserved or remote areas. Hybrid methods that integrate multiple AI techniques have further improved performance in image classification and feature extraction.

This chapter presents an overview of skin diseases in humans and animals, along with a review of AI-based diagnostic approaches, focusing on ML, DL, and hybrid models.

2. Structure and Function of the Skin

2.1. Structure of the Skin

The skin, the largest organ of the body, plays a fundamental role as a protective barrier and physiological regulator. It actively contributes to maintaining homeostasis, protecting against external aggressions, and regulating body temperature. It is composed of three main layers: the epidermis, the dermis, and the hypodermis (also known as the subcutaneous tissue), each with specific and complementary structures and functions. **Figure 1** illustrates the anatomical structure of the skin, showing the epidermis (outer layer), dermis (middle layer), and hypodermis (deep layer), along with associated structures such as hair follicles, glands, and blood vessels.

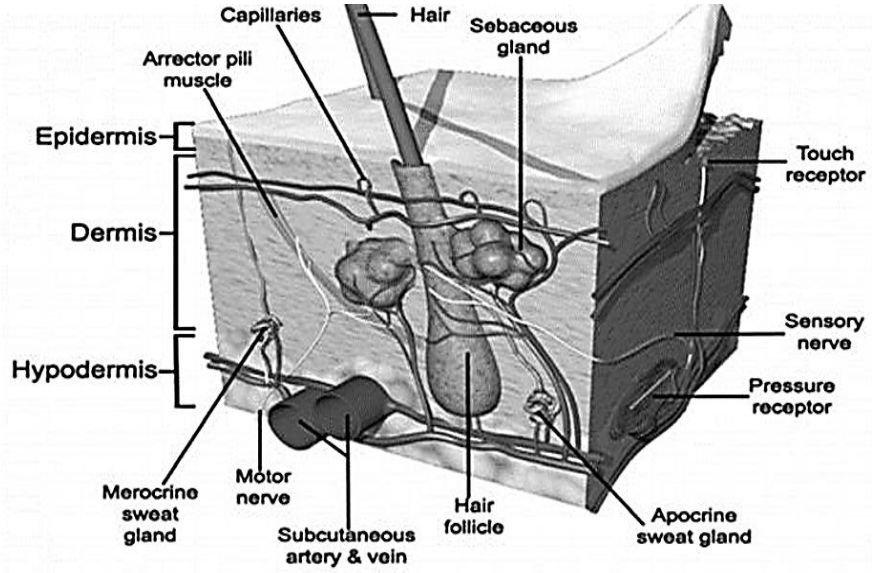


***Figure 1**: Diagram of the three main layers of the skin (epidermis, dermis, hypodermis) [01]*

2.1.1 The Epidermis

The epidermis is the outermost layer of the skin and serves as the first line of defense against environmental aggressions. It is primarily composed of keratinocytes, which produce keratin an impermeable protein that provides strength and protection.

The epidermis is divided into several strata, each playing a specific role [02]:

- **Stratum corneum:** Composed of dead, keratinized cells; forms a protective barrier against pathogens, chemicals, and water loss.
- **Stratum granulosum:** Cells in this layer produce lipids and proteins that reinforce the skin barrier.
- **Stratum spinosum:** Characterized by intercellular junctions called desmosomes, which provide mechanical strength.
- **Stratum basale:** The basal layer, containing stem cells responsible for epidermal renewal.

The epidermis also contains:

- **Melanocytes,** which produce melanin to protect against UV radiation;
- **Langerhans cells,** which play a role in immune defense.

Figure 2 depicts a zoomed-in view of the epidermal layers, showing the progression from the basal layer to the surface (stratum corneum), and highlighting the key cell types such as keratinocytes, melanocytes, and Langerhans cells.

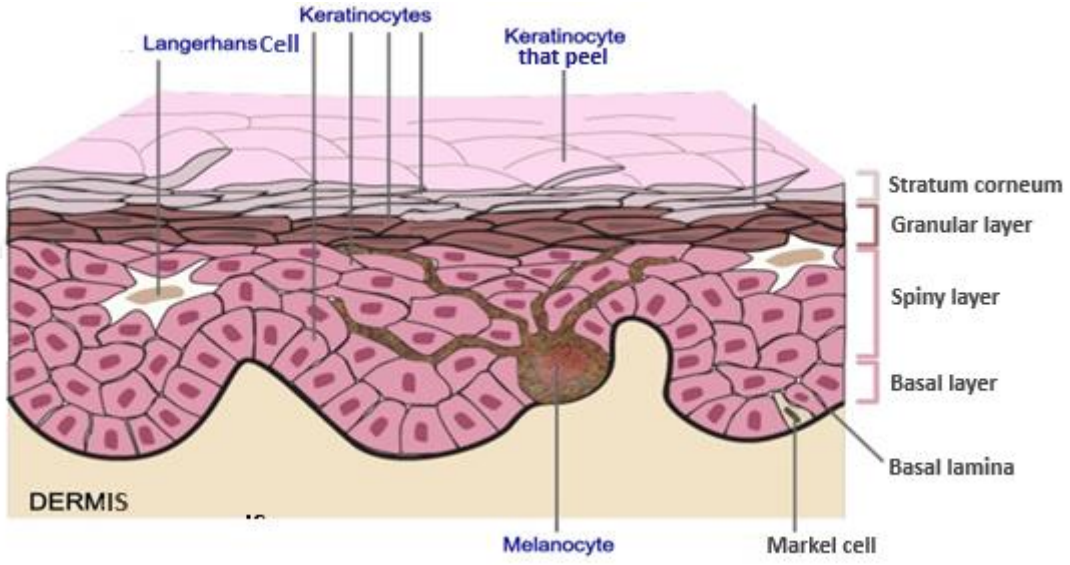


Figure 2: *Structure of the epidermis [03]*

2.1.2 The Dermis

The dermis, located just beneath the epidermis, is the intermediate layer composed of connective tissue rich in collagen and elastin, providing the skin with elasticity, strength, and flexibility.

It is divided into two regions:

- **Papillary dermis (superficial layer):** Contains blood capillaries that nourish the epidermis and sensory receptors.
- **Reticular dermis (deeper layer):** Denser in structure, it houses sweat glands, sebaceous glands, hair follicles, as well as blood vessels, nerves, and immune cells.

The dermis **[04]** plays a vital role in:

- Nourishing the epidermis,
- Sensory perception,
- Thermal regulation,
- Immune defense.

Figure 3. shows the two layers of the dermis (papillary and reticular), with key components like connective tissue, nerve endings, glands, and vascular networks illustrated in detail.

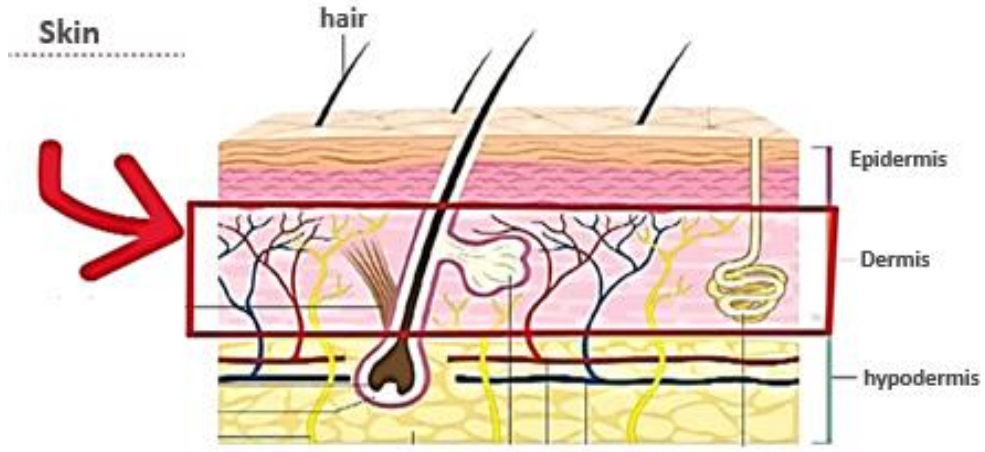


Figure 3: *Structure of the Dermis [05]*

2.1.3 The Hypodermis

The hypodermis, or subcutaneous tissue, is the deepest layer of the skin. Mainly composed of adipose tissue, it serves several functions [06]:

- Energy storage (lipid reserves),
- Thermal insulation,
- Mechanical protection of internal organs.

It also contains large blood vessels and nerves, connecting the superficial layers to the body's internal structures. The hypodermis provides mobility and flexibility to the skin, allowing it to adapt to bodily movements. Figure 4. highlights the adipose-rich composition of the hypodermis and its role in insulation, shock absorption, and as a structural link between the skin and underlying muscles/organs.

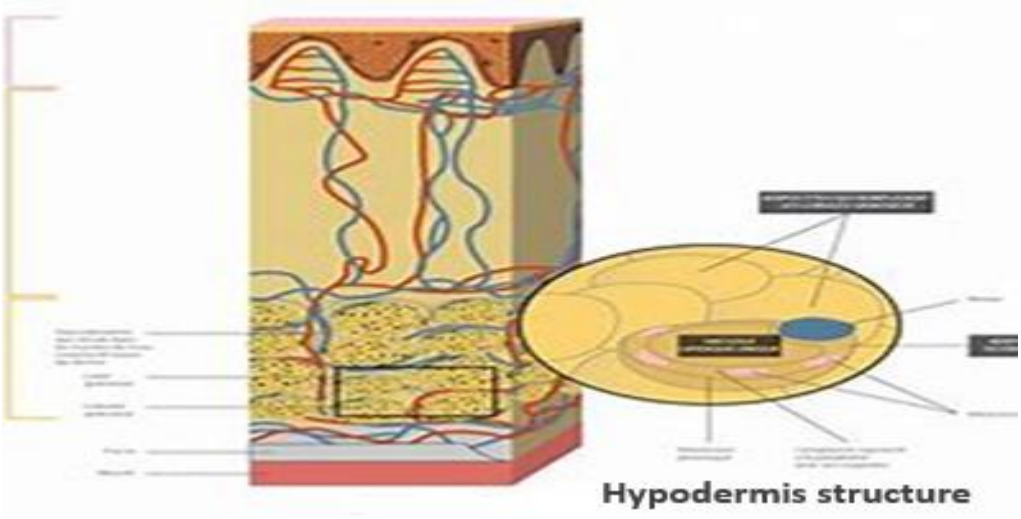


Figure 4*:Structure of the hypodermis [07]*

Together, these three layers work in close cooperation to ensure the skin's vital functions: protection, thermal regulation, sensation, immune defense, and homeostasis. In animals, specific adaptations (such as fur, feathers, or scales) enhance these functions but also make the skin susceptible to certain diseases. A thorough understanding of this architecture is essential for the diagnosis and treatment of skin conditions particularly with the aid of emerging technologies such as machine learning.

2.2 Functions of the Skin

The skin is far more than a simple outer covering; it plays a vital role in maintaining the body's physiological balance. Its functions are numerous and interdependent, made possible by the complex structure of its three layers**[08]**.

2.2.1 Protective Function

The skin serves as a multifunctional barrier essential for survival**[08]**:

- **Physical barrier:** Protects against pathogens (bacteria, viruses, fungi), irritating chemicals, and mechanical trauma.
- **Water barrier:** Limits transepidermal water loss, preserving the body's hydration.
- **Photoprotective barrier:** Melanocytes produce melanin, a pigment that absorbs ultraviolet (UV) rays, reducing cellular damage and genetic mutations caused by sun exposure.

2.2.2 Thermoregulation

The skin plays a key role in maintaining body temperature**[09]**:

- **Sweat evaporation:** Sweat glands secrete sweat; its evaporation helps dissipate excess heat**[09]**.
- **Vascular regulation:** Blood vessels in the dermis dilate (vasodilation) to promote heat loss or constrict (vasoconstriction) to retain heat**[09]**.
- **Thermal insulation:** Adipose tissue in the hypodermis acts as an insulating layer, limiting heat loss.

2.2.3 Sensory Perception

The skin is a major sensory organ, richly innervated to perceive environmental stimuli**[09]**:

- **Light touch:** Detected by Meissner's corpuscles in the papillary dermis.
- **Deep pressure and vibrations:** Perceived by Pacinian corpuscles, located deeper in the dermis.
- **Pain:** Transmitted by nociceptors (free nerve endings sensitive to harmful stimuli).
- **Temperature:** Detected by thermoreceptors.

2.2.4 Excretion and Secretion

The skin helps eliminate waste and maintain the skin's hydrolipidic barrier**[10]**:

- **Excretion:** Sweat glands eliminate urea, mineral salts, and toxins.
- **Secretion:** Sebaceous glands produce sebum, which:
    - Forms a hydrolipidic film,
    - Maintains hydration,
    - Inhibits microbial growth.

2.2.5 Immune Defense

The skin is part of the innate immune system and serves as an active immunological barrier**[10]**:

- **Langerhans cells**, present in the epidermis, detect antigens and activate local or systemic immune responses.
- **Skin pH** (around pH 5.5) creates an environment that is unfavorable for the proliferation of pathogenic microorganisms.

2.2.6 Vitamin D Synthesis

Under exposure to sunlight (UVB rays) **[10]**:

- **7-dehydrocholesterol**, present in the epidermis, is converted into **pre-vitamin D3**, which is then transformed into active **vitamin D (calcitriol)** by the liver and kidneys.
- This vitamin is essential for the **absorption of calcium and phosphorus**, **bone mineralization**, and the **proper functioning of the immune system**.

3. Overview of Skin Diseases

Skin diseases are dermatological conditions that affect both humans [11] and animals [12]. They have varied etiologies, including infectious agents (bacterial, fungal, viral, parasitic), autoimmune disorders, allergic reactions, and hormonal imbalances. Depending on their severity, these conditions can have aesthetic, functional, or even life-threatening consequences.

3.1 Skin Diseases in Humans

3.1.1 Infectious Diseases

Infectious skin diseases are caused by pathogenic microorganisms and can vary widely in severity, transmission mode, and clinical presentation. These conditions may be localized or systemic, and accurate diagnosis is essential for effective treatment**[13]**.

➢ **Bacterial Infections:**

- **Impetigo:** A highly contagious superficial skin infection primarily caused by *Staphylococcus aureus* or *Streptococcus pyogenes*. It presents as weeping, crusty lesions, often around the mouth and nose, mostly affecting children**[13]**.
- **Erysipelas:** An acute infection of the dermis characterized by well-defined, painful redness, often accompanied by fever. It is usually caused by *Streptococcus pyogenes***[13]**.
- **Cellulitis:** A deeper infection of the skin and subcutaneous tissues, caused by *Staphylococcus* or *Streptococcus*, typically originating from a breach in the skin**[13]**.

➢ **Fungal Infections:**

- **Ringworm (*Tinea corporis, Tinea capitis*):** Dermatophytoses caused by keratinophilic fungi (*Trichophyton, Microsporum*)**[13]**, resulting in annular, scaly, and itchy lesions.
- **Cutaneous Candidiasis:** Caused by *Candida albicans*, it affects moist areas (e.g., skin folds), producing erythema, maceration, and whitish patches**[13]**.

➢ **Viral Infections:**

- **Herpes Simplex (HSV-1, HSV-2):** Causes painful vesicular lesions on the skin or mucous membranes**[13]**.
- **Shingles (*Herpes zoster*):** A reactivation of the varicella-zoster virus, leading to painful, unilateral eruptions along a dermatome**[13]**.
- **Cutaneous Warts:** Caused by human papillomaviruses (HPV), typically appearing on the hands, feet, or genital area**[13]**.

➢ **Parasitic Infections:**

- **Scabies:** Caused by *Sarcoptes scabiei*, it results in severe nocturnal pruritus and characteristic burrows in the skin**[13]**.
- **Cutaneous Leishmaniasis:** Transmitted by sandflies (*Phlebotomus*), it causes chronic, painless ulcers.

3.1.2 Inflammatory and Autoimmune Diseases

- **Psoriasis:** A chronic autoimmune condition marked by erythematous plaques covered with silvery scales, often located on the elbows, knees, and scalp**[13]**.
- **Eczema (Atopic Dermatitis):** A chronic inflammatory skin disease characterized by dry skin, intense itching, and an allergic predisposition**[13]**.

- **Cutaneous Lupus Erythematosus:** A cutaneous form of systemic lupus erythematosus, associated with a butterfly-shaped rash on the face and photosensitivity**[13]**.

3.1.3 Allergic and Environmental Diseases

- **Urticaria (Hives):** A transient eruption of itchy wheals due to histamine release, typically triggered by allergens.
- **Contact Dermatitis:** An inflammatory reaction following exposure to allergens (e.g., nickel, latex) or irritants (e.g., chemicals, plants).

3.2 Skin Diseases in Animals

3.2.1 Infectious Diseases

➢ **Bacterial Infections:**

- **Bacterial Pyoderma:** Common in dogs and cats, mainly caused by *Staphylococcus pseudintermedius*, often secondary to allergies or parasitic infestations **[14]**.
- **Dermatophilosis:** Caused by *Dermatophilus congolensis*, this disease affects horses, cattle, and sheep, resulting in thick crusts and suppurative lesions **[15]**.

➢ **Fungal Infections:**

- **Animal Ringworm (*Microsporum canis*, *Trichophyton*):** A contagious zoonotic infection producing circular, hairless lesions **[14]**.
- **Cutaneous Candidiasis in Animals:** Rare, typically occurring under conditions of moisture or immunosuppression**[15]**.

➢ **Viral Infections:**

- **Viral Papillomatosis:** Benign warts caused by papillomaviruses, seen in dogs, cattle, and horses**[16]**.
- **Sheep and Goat Pox:** A serious viral disease characterized by fever, pustular skin lesions, and tissue necrosis**[16]**.

➢ **Parasitic Infections:**

- **Sarcoptic Mange (*Sarcoptes scabiei* var. *canis/bovis*):** Highly pruritic and contagious, with zoonotic potential**[17]**.
- **Demodectic Mange (*Demodex canis/cati*):** Causes localized or generalized alopecia, often with secondary infections**[15]**.

3.2.2 Autoimmune and Allergic Diseases

- **Pemphigus Foliaceus:** A rare autoimmune skin disorder in domestic carnivores, characterized by blisters, crusts, and erosions**[18]**.

- **Flea Allergy Dermatitis (FAD):** A hypersensitivity reaction to flea saliva, leading to intense pruritus**[15]**.
- **Canine Atopy:** An allergic reaction to environmental allergens (dust mites, pollen), causing chronic itching and secondary infections**[19]**.

3.2.3 Hormonal and Metabolic Diseases

- **Canine Hypothyroidism:** Results in a dull coat, symmetrical non-pruritic alopecia, and increased susceptibility to infections**[15]**.
- **Cushing's Syndrome (Hyperadrenocorticism):** Manifests as skin thinning, bilateral alopecia, comedones, calcinosis cutis, and recurrent infections**[15]**.
- **Cutaneous Dirofilariasis:** A mosquito-borne infection (*Dirofilaria repens*), forming migratory subcutaneous nodules**[15]**.

4. Current Challenges in Diagnosing Skin Diseases

The diagnosis of skin diseases traditionally relies on a combination of clinical observation, laboratory tests (e.g., biopsy, culture, histopathology), and the expertise of healthcare professionals or veterinarians. However, this approach presents several key limitations:

- High cost of specialized tests
- Slow turnaround times, especially for lab analyses
- Limited access in rural or under-resourced areas
- Heavy reliance on human expertise
- Symptom overlap across diseases, complicating differential diagnosis

These challenges underscore the need for diagnostic tools that are faster, more accessible, affordable, and accurate particularly through the application of artificial intelligence (AI).

5. Background and Problem Statement

Dermatological diseases are common in both humans and animals and require rapid and reliable diagnosis to ensure effective treatment and prevent complications. However, conventional diagnostic approaches often fall short, especially in resource-constrained or rural veterinary contexts.

Machine learning (ML) and deep learning (DL) technologies offer promising alternatives. By leveraging large datasets of medical images, these models can detect morphological patterns, textures, and colors with accuracy comparable to, or exceeding, that of human specialists.

5.1 Machine Learning

Machine Learning (ML) is a branch of artificial intelligence that enables computers to learn from data without explicit programming. Using training datasets, ML algorithms construct models capable of recognizing patterns, establishing correlations, and making predictions.

This approach is well-suited to complex tasks such as automated classification of skin diseases from images tasks that would be difficult to solve through handcrafted rules [30].

Common ML Techniques:

- **Support Vector Machines (SVM):** Effective supervised classifiers for binary or multiclass problems; they maximize the margin between classes in high-dimensional spaces [21].
- **Random Forests:** An ensemble method using multiple decision trees; robust to noise and overfitting due to majority voting.
- **k-Nearest Neighbors (k-NN):** A non-parametric algorithm that classifies a sample based on its k nearest neighbors; popular in medical imaging for its simplicity and effectiveness on small datasets [21].

5.2 Deep Learning

Deep Learning (DL), a subfield of ML, utilizes multi-layered neural networks to model complex, nonlinear relationships. Unlike traditional ML methods, DL performs automatic feature extraction directly from raw data, making it especially effective in medical image analysis [21].

Common DL Architectures:

- **Convolutional Neural Networks (CNNs):** Tailored for image analysis, they extract local features such as edges and textures. CNNs are widely used for classification, segmentation, and detection of skin lesions [21].
- **Autoencoders:** Unsupervised neural networks used for dimensionality reduction, information compression, and feature learning. Often integrated into hybrid models for enhanced performance [21].

5.3 Hybrid Approaches

Hybrid approaches in artificial intelligence combine several paradigms, including:

- Machine Learning techniques (SVM, Random Forest, k-NN),
- Deep Learning architectures (CNN, DNN, autoencoders),
- and even human expertise to guide or correct the models.

This methodological fusion aims to leverage the strengths of each approach while mitigating their specific weaknesses. Hybrid systems thus offer:

- improved diagnostic accuracy,
- reduced overfitting,
- better generalization on heterogeneous datasets,
- and increased interpretability of results, a valuable asset in the medical field [22].

6. Conclusion

Timely and accurate diagnosis of skin diseases is vital for guiding appropriate treatment and minimizing complications in both humans and animals. While traditional methods remain essential, they are limited by accessibility, cost, and diagnostic complexity.

Advances in artificial intelligence particularly in ML and DL hold significant promise for developing automated, fast, and reliable diagnostic tools. These models can analyze large volumes of dermatological images and detect subtle patterns often missed by the human eye.

This chapter has provided an overview of common human and animal skin diseases, current diagnostic challenges, and AI-based solutions. The next chapters will explore in detail the most widely used ML and DL models in dermatology, along with performance evaluations across various datasets.

Chapter 2 : Rlated Work

1. Introduction

The automation of dermatological pathology identification is currently a rapidly developing field of study, both in the medical and veterinary domains. The heterogeneity and complexity of skin conditions, combined with a limited number of specialists in certain geographical areas, make classical diagnosis difficult and sometimes inaccessible. In this context, artificial intelligence technologies, notably Machine Learning (ML) and Deep Learning (DL), show promising potential to help healthcare professionals quickly and accurately identify these diseases.

The application of these techniques to the analysis of dermatological images promotes the automation of lesion detection and classification by leveraging discriminative image features. In scientific publications, many methods can be found, ranging from traditional supervised learning techniques that rely on manual feature extraction (such as shape, texture, and color) to deep neural networks capable of automatically learning sophisticated representations from large datasets. There are also so-called hybrid methods, which combine the strengths of both paradigms to optimize classification performance.

2. Related Work

This section presents a thorough review of recent research on the detection of skin conditions from medical images, whether human or animal. The analysis is structured according to the methodological approaches employed (machine learning, deep learning, or hybrid methods), the datasets used, the evaluation protocols applied, as well as the reported performance metrics (accuracy, recall, F1-score, etc.). The objective is to highlight current trends, persistent limitations, and major contributions in order to position our own study within a coherent and well-justified methodological framework.

2.1. Classical Machine Learning-Based Approaches

In this subsection, we present two approaches based on classical Machine Learning techniques, detailed as follows:

Kumar et al. (2023) [23] propose an approach based on multiple machine learning models for predicting Lumpy Skin Disease (LSD) in cattle. Their method involves a comparative

evaluation of various classification and regression algorithms, including Random Forest (RF), Polynomial Features (Poly-F), Decision Tree (DT), k-Nearest Neighbors (K-NN), among others.

The study uses a public dataset composed of 14 attributes, split with a 70% training and 30% testing ratio, employing 10-fold cross-validation (k=10) to ensure the robustness of results. Model performances are evaluated using standard metrics such as accuracy, mean absolute error (MAE), mean squared error (MSE), and root mean squared error (RMSE).

Among the tested models, Random Forest stands out with superior performance, achieving an accuracy of 97.10%, MAE of 0.028, MSE of 0.028, and RMSE of 0.017. The Poly-F model closely follows with an accuracy of 96.77%. The authors emphasize the potential of these models for early LSD diagnosis and suggest that integrating deep learning could further enhance accuracy and generalizability. This work fully fits within the field of artificial intelligence applied to veterinary medicine, illustrating the effectiveness of traditional machine learning methods in combating animal diseases with significant health and economic impact.

Similarly, **Olaniyan et al. (2023)** [24] proposed an efficient predictive model for detecting LSD in cattle and buffaloes by combining classical machine learning techniques with optimized artificial neural networks (ANNs). Their approach includes advanced feature selection using the FeatureWiz method to eliminate redundant and irrelevant meteorological and geospatial data. Two models are implemented: a stacked ensemble model and an ANN.

The ensemble model combines four base classifiers (RF, DT, K-NN, and SVM) with logistic regression as the meta-classifier. The ANN model is based on a sequential architecture including fully connected (dense) layers, the ReLU activation function, and the Adam optimizer. The authors tested their models on a dataset of 24,803 instances, split 70/30 for training and testing. Results demonstrate an accuracy of 98.44%, recall of 98.68%, and F1-score of 98.93% for the ensemble model, while the optimized ANN achieves an accuracy of 98.89% after 200 epochs. These performances surpass those of a previous ANN model (97% accuracy), highlighting the relevance of the approach for early detection of LSD, a viral disease with high economic impact. This work belongs to the domain of classical machine learning enhanced by targeted neural network optimization, constituting a valuable

contribution to the agricultural and veterinary fields, especially regarding epidemiological surveillance of animal diseases [24].

2.2. Deep Learning (DL)-Based Approaches

In this subsection, we present several approaches based on deep learning techniques, described in detail below:

Wei et al. (2023) [25] propose an advanced method for skin disease classification by combining two state-of-the-art architectures: DenseNet201 and ConvNeXt_L. Their strategy relies on a dual feature extraction process, leveraging both intermediate layers (shallow features) and final layers (deep features) for a multi-level representation of lesions. Two attention modules are integrated to enhance the relevance of the extracted features: Efficient Channel Attention (ECA), which dynamically weights the most informative channels, and Global Context Transformer (GCT), which captures the global context of the image. The feature vectors from the two models are fused and then passed through a fully connected layer followed by a Softmax for classification.

Evaluated on a private dataset (2,600 images, 4 classes) and the public HAM10000 dataset (10,015 images, 7 classes), the approach achieves accuracies of 96.54% and 95.29%, respectively, with an F1-score reaching up to 89.99%, demonstrating strong robustness. This study is based on human data and fits within a purely convolutional approach enhanced by attention mechanisms.

Rao et al. (2021) [26] developed an automatic skin disease detection system using a convolutional neural network (CNN) built with Keras. The model classifies dermatoscopic images into seven main categories from the HAM10000 dataset (10,010 images), following preprocessing steps including cleaning, transformation, and exploratory analysis. The CNN architecture consists of Conv2D layers, MaxPooling2D, ReLU activations, dropout, and fully connected layers, optimized using the Adam algorithm. Training over 50 epochs yielded an accuracy of 93.35% and a loss of 15.65%, highlighting the relevance of this approach for multiclass classification. Although the system does not replace medical diagnosis, it represents a promising support tool in the field of deep learning applied to human dermatology.

Li et al. (2020) [27] conducted an exhaustive review of 45 studies published between 2016 and 2020 on the use of deep learning for skin disease detection. They compared the

performance of classical CNN models (AlexNet, VGG, Inception, ResNet, DenseNet), hybrid approaches, and multimodal techniques. Emphasis was placed on the importance of preprocessing (cleaning, artifact removal, normalization) and data augmentation (through rotation or GANs) to address class imbalances in datasets such as ISIC and HAM10000. Deep learning models outperform traditional methods, achieving accuracies up to 93.35% and AUCs reaching 98.1% through model fusion. The authors identify future challenges including synthetic data generation, adaptation to diverse clinical photographs, explainability of decisions, and mobile integration for diagnostics. This review demonstrates the transformative potential of AI in personalized dermatology.

Mujahid et al. (2024) [28] hey focus on the detection of viral skin diseases in animals, such as monkeypox, chickenpox, and Lumpy Skin Disease (LSD). Their model is based on DenseNet-169 coupled with the CBAM attention module, enhanced by synthetic image generation via DCGAN to compensate for the small dataset size (205 initial images). The augmented dataset is used for training with a 70/30 split, achieving an accuracy of 99.11%, an F1-score of 99.08%, and a recall of 98.89%. The combination of attention mechanisms, GAN-based generation, and DenseNet architecture demonstrates remarkable effectiveness in a limited-data context, focused exclusively on animal health.

Hwang et al. (2022) [29] proposed an innovative method for the classification of canine skin diseases using **images captured by a multispectral imaging device**. The study collected 95 clinical images of dog skin, categorized into four classes: bacterial dermatosis, fungal infections, hypersensitivity allergic dermatosis, and healthy skin. Four well-established CNN architectures (InceptionNet, ResNet, DenseNet, and MobileNet) were used to train models on both normal and multispectral images. The authors then developed a **consensus model** that combined the best-performing normal and multispectral models. This fused model achieved **89% accuracy** and a **Matthews Correlation Coefficient (MCC) of 0.76** for bacterial dermatosis classification, outperforming the individual models. The study highlights the value of **multispectral imaging**, which helps reveal skin redness not visible to the naked eye, and confirms the relevance of deep learning combined with spectral data for veterinary diagnostics, even on small datasets. This work contributes meaningfully to the field of intelligent systems for animal health monitoring**Senthilkumar et al. (2024)** [30] compare ten pre-trained CNN models for detecting Lumpy Skin Disease (LSD) in cattle. Using transfer learning on two public datasets enriched with images of other pathologies (dermatophilosis,

ringworm, etc.), the authors optimize performance through standard data augmentation and tailored fine-tuning. MobileNetV2 achieves an accuracy of 96.39% with a specificity of 100%, while VGG16 obtains an accuracy of 96.07% and a sensitivity of 93.75%. These results outperform classical methods (SVM, MLP) and underline the usefulness of such tools for rapid diagnosis, particularly in rural settings.

Bajwa et al. (2020) [31] explore a deep network–based approach for the automated diagnosis of human dermatological diseases. Using two large datasets (DermNet: 21,844 images; ISIC Archive: 23,665 images), the authors evaluate several pre-trained CNNs (ResNet-152, DenseNet-161, SE-ResNeXt-101, NASNet), optimized through fine-tuning. A hierarchical strategy enhances performance on the 622 subclasses of DermNet, achieving a Top-1 accuracy of 66.74%. For the superclasses, results reach 79.94% (Top-1) and 95.02% (Top-5), with an AUC of 98.07%. This study demonstrates the effectiveness of deep neural networks (DNNs) for large-scale fine-grained classification, despite limitations related to variable image quality and the absence of clinical metadata.

2.3. Hybrid Approaches

This subsection is dedicated to presenting various hybrid approaches that combine traditional machine learning and deep learning, described in detail in the following paragraphs.

Sun et al. (2023) [32] present a comprehensive review of deep learning technologies applied to skin disease recognition. The study highlights the performance of classical CNN architectures such as ResNet, VGG, AlexNet, DenseNet, and GoogleNet, while emphasizing the importance of encoder-decoder models like U-Net for lesion segmentation. These models are primarily trained on standard datasets such as ISIC, HAM10000, PH2, and Dermofit. The authors stress the necessity of rigorous preprocessing (contrast enhancement, noise removal, normalization), as well as precise lesion segmentation, since these steps directly influence classifier performance. Models incorporating a prior segmentation step achieve AUCs greater than 0.98 and accuracies up to 99.5%. Moreover, the article highlights the growing interest in multimodal approaches that combine several CNNs in parallel to exploit their complementarity. This work, focused exclusively on human data, is fully situated within the deep learning framework, underscoring the central role of segmentation in the analysis pipeline [32].

Said and Rhaimi (2024) [33] propose an integrated approach to improve the early detection of melanoma from dermoscopic images. Aware of the challenges posed by the variability of skin lesions—such as blurred contours, irregular shapes, color variations, and complex structures—they present a model based on a combination of advanced image processing, feature extraction, and classification techniques. The preprocessing phase relies on adaptive histogram equalization, which enhances image clarity by reducing artifacts such as shadows, hair, and lighting differences. For feature extraction, several methods are used jointly: the ABCD rule (Asymmetry, Border, Color, Diameter), texture descriptors based on the gray-level co-occurrence matrix (GLCM), Histogram of Oriented Gradients (HOG), and deep autoencoders derived from deep learning. Classification is performed through an ensemble approach combining convolutional neural networks (CNNs) and support vector machines (SVMs), leveraging transfer learning from pre-trained models in a multi-class setting. This architecture aims to increase detection accuracy, reduce costs associated with manual medical expertise, and improve ease of clinical integration. The proposed model is designed to be continuously evaluated using updated datasets, thereby ensuring its robustness and effectiveness over time [33].

Mahum and Aladhadh (2022) [34] propose an innovative hybrid approach for the automatic detection of melanoma, combining classical feature extraction techniques with deep learning methods. Their methodology begins with manual feature extraction using the Local Binary Pattern (LBP) descriptor, which is effective at capturing local textures. In parallel, deep features are extracted via the InceptionV3 model, a CNN pre-trained on ImageNet, capable of identifying complex patterns at multiple scales. These two types of features are fused through an entropy-based selection method that retains only the most discriminative attributes. This fused feature set is then fed into an LSTM (Long Short-Term Memory) model, used here as a sequential classifier to capture the structure and correlations between descriptors. Evaluated on a dataset of 1,000 images from the DermIS dataset (700 for training and 300 for testing), the system achieves an accuracy of 99.4%, precision of 98.7%, recall of 98.66%, and F1-score of 98.6%. This approach, applied to human data, demonstrates the effectiveness of a hybrid system combining classical machine learning and deep learning for robust skin cancer detection [34].

Debelee (2023) [35] presents a comprehensive systematic review on the automatic identification of skin diseases using artificial intelligence. The study analyzes 45 recent

articles, covering multiple methodological dimensions: the type of approach (machine learning, deep learning, or hybrid), types of extracted features (texture, shape, color, deep features), classifiers employed (SVM, Random Forest, CNN, etc.), utilized datasets (ISIC, HAM10000, DermIS, PH2, etc.), and preprocessing techniques (normalization, noise reduction, segmentation, data augmentation). The author highlights the superiority of hybrid approaches that combine handcrafted descriptors (e.g., LBP, GLCM) with deep features extracted from CNNs, achieving classification rates up to 99.94%. The study also emphasizes the critical role of segmentation in enhancing performance, as well as the emerging trend toward multimodal architectures and Transformer-based networks. Focused on human skin data, this work provides a valuable overview and underscores the field's evolution toward smarter and more reliable hybrid systems [35].

3. Main Datasets

This subsection presents in detail several datasets dedicated to the study of skin diseases, whose characteristics are described below.

- **DermIS (Dermatology Information System) [36]** is an online dataset developed for educational purposes by German dermatologists. It contains over 10,000 dermatological images covering a wide range of human skin conditions, such as psoriasis, fungal infections, viral warts, basal cell carcinoma, and malignant melanoma. Most of the images are standard clinical photographs taken without specialized equipment, making them particularly representative of conditions encountered in everyday medical practice.

  Each image is typically accompanied by a textual diagnosis, sometimes enriched with clinical notes or medical articles. However, the unstructured format of these annotations limits their direct use in supervised classification approaches. Moreover, the image quality varies significantly in terms of lighting, resolution, and framing, requiring extensive preprocessing (normalization, cleaning, data augmentation) before use.

  Despite these limitations, DermIS remains a valuable resource, especially for traditional machine learning models. It is frequently used in comparative studies or as an initial training dataset for models designed to handle heterogeneous image collections.
- **The ISIC (International Skin Imaging Collaboration) dataset [37]**, developed as part of an international collaborative project, is one of the most reliable and widely

used dermatological datasets for AI-assisted detection research. It contains over 33,000 high-resolution dermoscopic images annotated by expert dermatologists.

Each image is accompanied by a clinical diagnosis—sometimes histopathologically validated—as well as accurate segmentation masks and relevant metadata (e.g., sex, age, and anatomical location). The dataset covers multiple classes of skin conditions, including benign nevi, melanoma, actinic keratosis, basal cell carcinoma, and other pigmented or non-pigmented lesions.

Regularly updated, especially through international competitions such as the ISIC Challenge [37], this dataset has become a benchmark for evaluating deep learning models, particularly convolutional neural networks (CNNs), segmentation architectures (such as U-Net and DeepLab), and hybrid approaches combining image analysis with machine learning techniques.

Thanks to its exceptional image quality, rich annotations, and broad range of skin conditions, ISIC is a key resource for the development and validation of automated dermatological diagnostic systems.

- **The LSD (Leeds Skin Dataset) [38]**, developed by the University of Leeds, is a small yet valuable resource for skin lesion segmentation tasks. It contains approximately 200 to 300 clinical images, primarily of pigmented lesions such as nevi and melanomas, captured in a controlled medical environment.

  One of its key strengths lies in the availability of high-precision manual segmentation masks, accurately outlining the lesion area in each image. These rigorous annotations make the dataset particularly suitable for training segmentation models, including convolutional architectures such as U-Net, Mask R-CNN, and Fully Convolutional Networks (FCNs).

  However, the dataset has certain limitations: it covers a limited number of pathological classes, suffers from data imbalance, and lacks patient metadata (e.g., age, sex, anatomical location). As a result, it is rarely used for multi-class classification tasks but remains a reliable reference for evaluating performance in supervised segmentation.

  Additionally, the clinical (non-dermoscopic) images in the LSD dataset complement those from other datasets such as ISIC or HAM10000, which focus more heavily on dermoscopic imaging.

- **HAM10000 (Human Against Machine with 10,000 training images) [39]** is a major dermatological dataset composed of 10,015 dermoscopic images, made

available by the Medical University of Vienna. Specifically designed for research on automated skin lesion classification, this dataset stands out due to its high construction quality and clinical diversity. The images were collected from two distinct clinical sources, then cleaned, verified, and rigorously annotated by experienced dermatologists.

The dataset includes seven diagnostic categories representing the most common skin pathologies: benign nevi (nv), melanoma (mel), actinic keratoses and intraepithelial carcinoma (akiec), basal cell carcinoma (bcc), benign keratotic lesions (bkl), dermatofibroma (df), and vascular lesions (vasc).

Diagnoses are validated through histopathological examination, longitudinal clinical follow-up, or expert consensus, ensuring high annotation reliability. Each image is enriched with relevant metadata such as patient age, sex, and lesion anatomical location, enabling thorough contextual analyses.

Thanks to its semantic richness, significant size, and rigorous structuring, HAM10000 is widely used for training deep learning models, especially convolutional neural networks (CNNs) like ResNet50, InceptionV3, and EfficientNet. It also serves as an ideal case study for hybrid approaches combining manual feature extraction and automatic classification.

Furthermore, its class imbalance makes it an excellent benchmark for evaluating the robustness of algorithms under realistic conditions. As such, HAM10000 is now considered one of the most comprehensive and reliable open-access datasets for research in AI-assisted dermatological diagnosis.

- **DermNet [40]**, more precisely DermNet NZ, is a reference educational platform developed and managed by a team of New Zealand dermatologists. It offers thousands of high-resolution clinical images covering a wide spectrum of dermatological conditions, ranging from common ailments (e.g., acne, eczema, bacterial infections, contact dermatitis) to rarer diseases (e.g., lupus, atypical skin tumors). Unlike standardized datasets such as ISIC or HAM10000, DermNet was not specifically designed for algorithmic research, but rather for educational purposes and public awareness. Nevertheless, its wide variety of images and their classification by diagnosis and skin type make it a valuable resource for building multiclass datasets or for studies focusing on ethnic variability in dermatology.

  However, DermNet presents several structural limitations: the images are not accompanied by automatically usable annotations (e.g., standardized formats like

XML or JSON), there are no segmentation masks, and patient metadata (e.g., age, sex, anatomical location) is generally absent.

As a result, integrating DermNet into machine learning projects requires substantial preprocessing and manual annotation work. Despite this, the dataset is frequently used as a complementary source, either to increase dataset diversity or to enrich the representativeness of realistic images in clinical detection systems.

- **The canine skin disease dataset**, published on the Mendeley Data platform in 2022 **[41],** consists of images captured using a multispectral imaging device. It is a valuable resource for the automated study of canine dermatological conditions using deep learning techniques. This dataset was specifically designed for the classification of multispectral images of dog skin, captured under real clinical conditions using a specialized device capable of recording information beyond the visible spectrum, particularly in the near-infrared. This approach helps reveal skin alterations invisible to the naked eye, thereby improving the discrimination between clinically similar but pathologically different lesions.

  The dataset contains 95 samples, divided into four diagnostic categories: 23 cases of bacterial dermatosis, 19 cases of fungal infection, 23 cases of allergic hypersensitivity reaction, and 30 cases of healthy dogs (control group).

  Each image is associated with a validated clinical annotation, allowing for reliable supervised classification. The data was collected in a professional veterinary setting with informed consent from the owners, ensuring both ethical and realistic acquisition conditions.

  From a technical standpoint, this dataset has been used to train and evaluate convolutional neural network (CNN) models, which have shown promising results in classifying the different conditions. Its high image quality, diversity of pathological classes, and rigorous annotations make it a reference tool in the still underexplored field of AI-assisted veterinary dermatology. In this master's thesis, this dataset is used as the primary corpus for training a canine skin disease classification model, in order to evaluate the performance of different deep learning approaches on real multispectral data.

4. Comparative Summary

The automatic identification of skin diseases—whether in humans or animals—has evolved significantly over the past decade. Initially, the field relied primarily on classical machine learning (ML) techniques, which required manual extraction of visual features such as texture, color, and shape. These features were then analyzed using traditional classifiers like Support Vector Machines (SVM), k-Nearest Neighbors (KNN), or Random Forest, yielding acceptable results in controlled environments. For example, Kumar et al. (2023) [23] applied methods such as SVM and Random Forest on tabular data to detect Lumpy Skin Disease (LSD), achieving an accuracy of 97.10%.

With the advent of deep learning (DL), the trend shifted toward convolutional neural networks (CNNs), which can automatically extract relevant features from raw images without the need for complex preprocessing. Numerous studies have explored advanced architectures such as VGG16, ResNet, DenseNet, MobileNetV2, and ConvNeXt, demonstrating remarkable performance. For instance, Senthilkumar et al. (2024) [30] achieved 96.39% accuracy in the early detection of LSD using an optimized CNN model, while Wei et al. (2023) **[25]** proposed a method that fused DenseNet and ConvNeXt_L with attention modules, achieving 95.29% accuracy on the HAM10000 dataset.

In parallel, hybrid approaches have emerged, combining the generalization power of deep learning with the simplicity and robustness of traditional ML algorithms. These strategies aim to maximize performance while reducing computational requirements. For example, Mahum and Aladhadh (2022) **[34]** combined Local Binary Pattern (LBP) descriptors with the InceptionV3 architecture and an LSTM classifier, achieving an accuracy of 99.4% on the DermIS dataset. Similarly, Olaniyan et al. (2023) [24] used an automated feature selection tool (FeatureWiz) in conjunction with traditional classifiers (e.g., artificial neural networks and stacking), reaching an accuracy of 98.66% for LSD detection.

Datasets vary according to the application domain. Studies on human skin diseases typically rely on well-established public repositories such as ISIC, HAM10000, DermNet, and DermIS. In contrast, research on animal skin diseases often depends on proprietary or custom-built datasets. Notably, the study by Hwang et al. (2022) **[29]** utilized multispectral imaging to detect canine dermatological diseases, achieving a Matthews correlation

coefficient (MCC) of 0.76—highlighting the value of alternative imaging modalities beyond the visible spectrum.

A comparative summary of the performance reported in these studies is presented in the table below:

Table 1 . Summary of Related Works on Skin Disease Detection

Authors	Type	Approach (Feature Extraction + Classification)	Dataset Used	Evaluation Protocol (Train/Test)	Classification Rate / Details
Bajwa et al. (2020) **[31]**	Human	ResNet-152, DenseNet-161, SE-ResNeXt, NASNet (ensemble learning, weighted CE)	DermNet (21k, 23 classes), ISIC 2018 (23k, 7 classes)	5-fold CV, adapted resolution	DermNet: 79.9% Top-1, ISIC: 93.1%, AUC up to 99.2%
Rao et al. **[26]**	Human	Preprocessing + CNN (Keras)	HAM10000 (10,010 images)	Train/Test (ratio not specified)	Accuracy: 93.35%, Loss: 15.65%
Wang et al. (2022) **[27]**	Human	Review (AlexNet, VGG, ResNet, fusion)	45 articles (various datasets)	Not applicable	Up to 99.5%
Wei et al. (2023) **[25]**	Human	DenseNet201 + ConvNeXt_L + ECA/GCT (attention modules)	Private dataset (2600), HAM10000	Private: 80/20, HAM10000: Test 828/2000	Accuracy: 96.54% (private), 95.29% (HAM), F1: 89.99%
Mujahid et al. (2024) **[28]**	Animal	DenseNet-169 + CBAM + DCGAN (augmentation)	205 images (3 pathologies)	75% train / 25% test	Accuracy: 99.11%, F1: 99.08%, AUC: 99.33%
Hwang et al. (2022) **[29]**	Animal	DenseNet +InceptionNet + Consensus Fusion	95 dogs(621 images multispectral)+ Normal images	85% train / 5% test/10% validation augmentation ×1000	MCC: 0.76, accuracy 85–90%
Senthilkumar et al. (2024) **[30]**	Animal	VGG16, ResNet, MobileNetV2, etc. + fine-tuning	LSD Dataset 1 (1024), Dataset 2 (2223)	70% train / 30% test	MobileNetV2: 96.39%, VGG16: 96.07%
Kumar et al. (2023) **[23]**	Animal	KNN, SVM, RF, DT, NB, Regression	Kaggle (tabular, 14 variables)	70% train / 30% test	RF: 97.10%, KNN: 95.09%
Olaniyan et al. (2023) **[24]**	Animal	FeatureWiz + stacking + ANN	LSD (24,803 entries)	70% train / 30% test	ANN: 98.66%, Stacked: 97.69%, F1: 98.93%
Sun et al. (2023) [32]	Animal	Review: U-Net, ResNet, attention, fusion	ISIC, HAM10000, PH2, etc.	Variable (depending on article)	Up to 99.5%, AUC > 0.98
Said & Rhaimi (2024) **[33]**	Animal	ABCD + GLCM + HOG + autoencoder +	Simulated images	Not specified	No quantified metrics

		CNN + SVM			
Debelee (2023) **[35]**	Animal	Review: CNN, SVM, hybrid CNN+SVM	ISIC, HAM10000, PH2, etc.	Variable (5-fold, 80/20, etc.)	Up to 99.94%
Mahum & Aladhadh (2022**) [34]**	Animal	LBP + InceptionV3 + LSTM	DermIS (1000 images)	700 train / 300 test	Accuracy: 99.4%, F1: 98%

Despite their excellent performance, deep learning models present certain limitations: they often require high computational resources and large volumes of annotated data to generalize effectively. To address these constraints, several complementary strategies have been proposed, including data augmentation using GANs, the incorporation of attention mechanisms (e.g., CBAM, ECA), and multi-level fusion techniques. For instance, Mujahid et al. (2024) integrated DenseNet-169 with CBAM and DCGAN to improve accuracy in detecting viral diseases in animals, reaching an impressive 99.11% accuracy.

This progression from traditional approaches to deep architectures and subsequently to hybrid models illustrates the maturation of the field. Current research increasingly focuses on enhancing generalization, mitigating bias, and developing lightweight models suitable for real-world applications in clinical, veterinary, and rural settings.

5. Conclusion

In this chapter, several studies on skin disease identification have been reviewed, with a focus on the diverse methodological approaches and their respective performances. This comparative analysis highlights a broad spectrum of techniques, ranging from classical machine learning models based on manual feature extraction to more recent deep learning methods capable of automatically learning relevant representations directly from images.

In addition, hybrid approaches that combine these two paradigms have also been explored, aiming to optimize both diagnostic accuracy and computational efficiency. These studies reflect a progressive shift towards more robust and intelligent systems, better adapted to the practical needs of both human and veterinary medicine.

However, challenges persist particularly in terms of model generalization, bias mitigation, and the seamless integration of these systems into clinical and rural environments. Continued efforts in these areas are crucial to improving early detection, reliable monitoring, and the effective management of skin diseases.

Chapter 3 : Experimental Evaluation and Results

1. Introduction

In recent years, the application of artificial intelligence techniques in the medical field has experienced significant growth, particularly in the classification of medical images. The classification of skin diseases in animals presents a major challenge, especially in rural areas where access to specialized veterinary care is limited. In this context, transfer learning plays a crucial role by enabling the reuse of models previously trained on large datasets, thereby accelerating training and improving performance in domains with limited data, such as the diagnosis of animal skin diseases.

This chapter evaluates the performance of a set of deep learning models based on transfer learning, using two types of input data: standard RGB images and multispectral images. It includes an explanation of the concept of transfer learning, details on data preparation, a presentation of the models used, training configurations, and a comprehensive analysis of the results obtained.

2. Tools and Libraries

The development of an automatic skin disease detection system using deep learning requires the integration of several specialized tools and libraries. These technologies manage the entire workflow—from the collection and preprocessing of medical images to the construction, training, evaluation, and visualization of model performance. The chosen tools were selected for their robustness, widespread use in the computer vision and deep learning communities, comprehensive documentation, and seamless interoperability.

2.1. Python

Python is the core programming language used in this project. Today, it is the standard in the field of artificial intelligence due to its simple syntax, low learning curve, and, most importantly, its rich ecosystem. Its dynamic nature supports rapid prototyping, while its integration with low-level libraries (written in C/C++) ensures high computational efficiency. In this thesis, Python was used to implement all modules: image import and preprocessing, CNN model construction, training, evaluation, and results visualization [42].



Figure 5: *Python Logo*

2.2. Kaggle

Kaggle played a dual role in this project. First, it provided access to high-quality, labeled datasets relevant to dermatological image classification. Second, its cloud-based environment—Kaggle Kernels—offered integrated GPU support, which was instrumental for training deep learning models efficiently without the need for local computational resources. This combination of reliable data access and scalable computing power made Kaggle an essential platform for both experimentation and implementation in this study [43].



Figure 6: *Kaggle Logo*

2.3. NumPy

NumPy is a fundamental library for numerical computation in Python. It enabled efficient manipulation of images in pixel matrix format. NumPy was used for key tasks such as pixel normalization (scaling values to the [0,1] range), reshaping arrays to fit model input dimensions, and generating binary masks for label processing. Its vectorized operations significantly enhanced performance by eliminating the need for slow, explicit loops [42].



Figure 7: *Numpy Logo*

2.4. Matplotlib

Visualizing data and model performance is essential in deep learning projects. **Matplotlib** was used to plot training curves (accuracy vs. epochs and loss vs. epochs), allowing for early detection of overfitting or underfitting. It was also employed to visualize image samples by class, confusion matrices for category-specific accuracy analysis, and model predictions. These visualizations provided meaningful insights that extended beyond numerical metrics [42].



Figure 8: *Matplotlib Logo*

2.5. Scikit-learn

Although deep learning formed the core of this project, **Scikit-learn** served as a valuable complementary tool. It was used to partition datasets into balanced training, validation, and test sets. It also provided built-in functions to compute evaluation metrics such as accuracy, recall, F1-score, and AUC (Area Under the ROC Curve). Additionally, it allowed for performance comparisons between deep learning models and traditional classifiers (e.g., SVM, KNN), thereby reinforcing the choice of CNNs in this medical application [42].



Figure 9: *Scikit-Learn Logo*

2.6. TensorFlow

TensorFlow was the main library used to implement deep learning models, particularly Convolutional Neural Networks (CNNs). It facilitates computational graph creation, automatic differentiation, GPU acceleration, and model serialization. In this project, TensorFlow enabled the design of CNNs capable of ingesting dermatological images, learning meaningful features (edges, textures, colors), and predicting their classes. Tools such as ModelCheckpoint, EarlyStopping, and custom callbacks were crucial for optimizing the training process [42].



Figure 10: *TensorFlow Logo*

2.7. Keras

Keras served as the high-level API for building CNN architectures intuitively and efficiently. It allowed for rapid development through predefined layers (e.g., Conv2D, MaxPooling2D, Dropout, Dense) and straightforward compilation using loss functions (e.g., categorical_crossentropy) and optimizers (e.g., Adam). Keras facilitated experimentation by enabling easy adjustments to model depth, filter sizes, and regularization parameters such as dropout. This flexibility was key to achieving optimal performance in an experimental setting [44].



Figure 11: *Keras Logo*

2.8. Jupyter Notebook

Jupyter Notebook is an open-source, web-based interactive environment that supports live code, equations, visualizations, and narrative text in a single document. It is widely used in data science and machine learning for exploratory data analysis, reproducible research, and collaborative development. In this project, Jupyter allowed seamless integration of code and documentation, improving the clarity and reproducibility of experimental workflows [45]

.

3. Description of the Dataset Used

The dataset used in this study is titled *"Classification of Pet Dog Skin Diseases Using Deep Learning with Images Captured from Multispectral Imaging Device"*, and is publicly available on the Mendeley Data platform [40]. It was specifically designed to support research into the automatic diagnosis of canine skin diseases using deep learning approaches.

A distinguishing feature of this dataset is its use of multispectral imaging, which captures images at multiple wavelengths—including infrared and ultraviolet—providing a richer and more informative representation than conventional RGB images.

General Characteristics:

- Total number of subjects: 95 dogs with a precise dermatological diagnosis at a veterinary clinic.
- Total number of images: Approximately 621 original images, with each dog contributing one RGB image and nine multispectral images. After data augmentation and multi-angle acquisition, the dataset was expanded to an estimated 31,050 images, reflecting roughly 50 variations per original image.
- Image dimensions used: generally resized to 128×128 pixels according to the requirements of the deep learning architectures used (e.g., DenseNet, Inception).
- Annotations: each image is labeled by a veterinary expert according to the diagnosed skin disease.

The dataset is categorized into four primary classes, each representing a specific skin condition. These classes, along with their descriptions and the number of dogs in each category, are summarized in Table 2.

Table 2 . Overview of Classes in the Multispectral Image Dataset

Class	Number of Dogs	Description
Bacterial Dermatoses	121	Infections caused by bacteria, typically characterized by lesions, pustules, and inflammation.
Fungal Infections	110	Mycotic infections of the skin, often manifesting as scaling, redness, and pruritus.
Allergic Dermatoses (Hypersensitivity)	130	Skin reactions due to allergens, presenting with inflammation and irritation.
Healthy Dogs (Control Group)	260	Images of healthy skin used as a reference for comparative classification.

4. Data Preprocessing and Dataset Splitting

Data preprocessing in this project begins with loading the multispectral images along with their corresponding labels, which are provided in a text file that maps each folder to a specific disease class. After parsing the label information, the images are organized into structured directories according to their class, facilitating efficient management and streamlined access.

Once this organization is completed, a DataFrame is created to store the file paths of the images along with their numerical labels. This tabular structure enables easy data manipulation and supports stratified splitting during subsequent stages.

The dataset is then divided into three subsetstraining, validation, and test using a stratified sampling approach to preserve the class distribution across all sets. The split follows a ratio of 70% for training, 15% for validation, and 15% for testing. To address potential class imbalance in the training data, class weights are automatically computed based on the distribution of samples per class. These weights are used during model training to ensure balanced learning.

Next, all images are preprocessed into a TensorFlow-compatible format. Each image is loaded and decoded based on its format, resized to a standard dimension of 128×128 pixels, normalized to a range of [0, 1], and batched to facilitate efficient training. This comprehensive preprocessing pipeline ensures optimal data quality and consistency, crucial for training a robust and high-performing convolutional neural network (CNN).

The dataset split is summarized in Table 3, which provides the number of images in each subset both before and after data augmentation:

Table 3 . Dataset Splitting and Preparation for Training

Subset	Percentage	Total Images (Original)	Total Images (After Augmentation)	Purpose
Training	70%	434	21,735	Model parameter optimization
Validation	15%	93	4,657	Performance monitoring during training
Test	15%	94	4,658	Final evaluation of generalization capability

5. Models Selection

In this study, we adopted a transfer learning approach to develop an efficient system for classifying skin diseases in dogs. Transfer learning leverages deep learning models pre-trained on large-scale datasets, such as ImageNet, to improve accuracy and significantly reduce training time particularly useful in scenarios with limited domain-specific data, such as veterinary dermatological images.

5.1. Transfer Learning

Transfer learning involves reusing knowledge acquired from a model trained on a source task to improve performance on a related target task. In our context, this means using models trained on millions of general-purpose images to classify canine skin conditions. These pre-trained models are highly effective at extracting generic features (such as textures, edges, and shapes) that can be fine-tuned for more specialized medical tasks.

Key advantages of transfer learning include:

- Reduced overfitting, especially with small datasets.
- Accelerated training time, as only a subset of layers needs to be retrained.
- Improved accuracy, due to the use of features already optimized for visual recognition.

5.2. Evaluated Pre-trained Models

To determine the most suitable model architecture for our application, we evaluated several well-established pre-trained convolutional neural network (CNN) models. These models span different architectural families, each with unique characteristics in terms of feature extraction, computational efficiency, and depth.

5.2.1 Architectural Families of Pre-trained Models

➤ ResNet (Residual Networks)

Introduced by He et al. in 2015 [46], Residual Networks (ResNet) addressed the degradation problem that occurs when training very deep networks. ResNet introduces **residual (or skip) connections** that allow gradients to flow more easily through the network during backpropagation. Instead of learning a direct mapping H(x), the network learns a residual function $F(x) = H(x) - x$, leading to the reformulated mapping:

$$H(x) = F(x) + x$$

These skip connections make it feasible to train much deeper models without performance loss. Figure 12 present Residual connections in ResNet architecture.

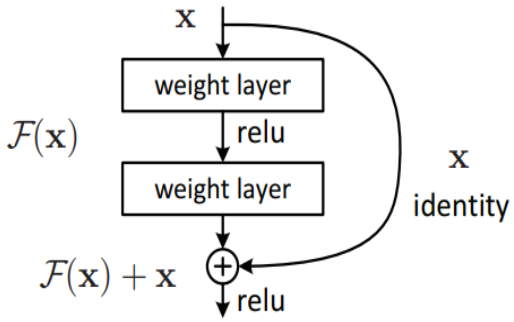


Figure 12: *Residual connections.[47]*

In this study, we experimented with:

- **ResNet50**: 50-layer network with residual connections.
- **ResNet101**: Deeper variant with 101 layers, capable of capturing more complex features.

➤ Inception Networks

The Inception architecture was introduced by Szegedy et al. as part of GoogLeNet (InceptionV1) [48]. Its core idea is to capture visual features at multiple scales simultaneously using parallel convolutional layers of different kernel sizes (1×1, 3×3, 5×5), combined with max-pooling operations. This makes the network particularly suited for images with varying spatial detail—common in skin lesion datasets. Figure13 show Inception block example.

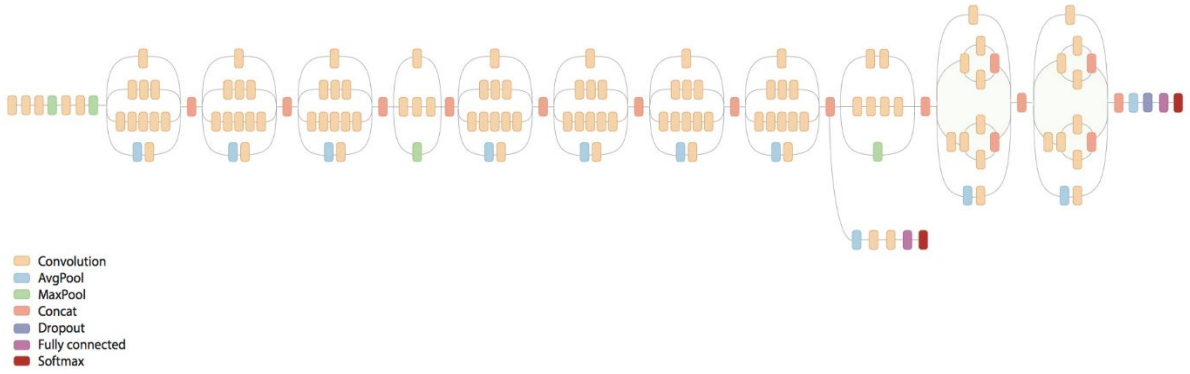


Figure 13: *Example of an Inception model [48]*

In this work, we employed InceptionV3, an optimized version of the original model. It includes the following improvements:

- Factorized convolutions: Large convolutions (e.g., 5×5) are decomposed into smaller ones (e.g., two 3×3), reducing computation.
- Extended batch normalization: Applied across most layers to accelerate and stabilize training.
- Regularization enhancements: The architecture is deeper but better structured, minimizing overfitting and improving generalization.

Figure14. depict an Example structure of InceptionV3 model

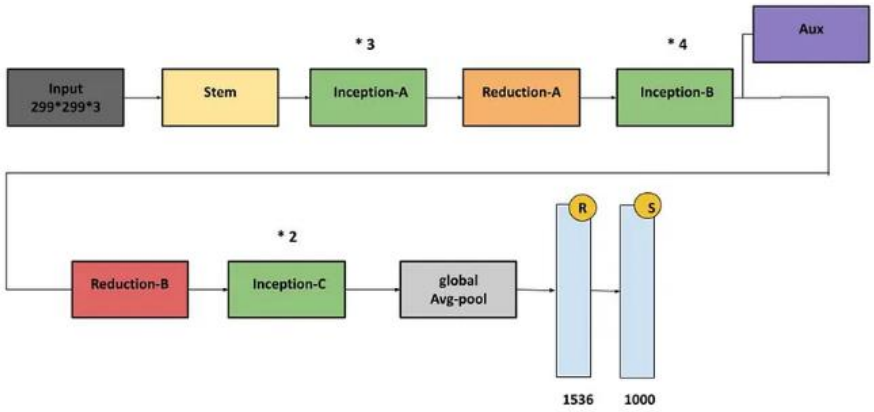


Figure 14: *Example of an InceptionV3 model [49]*

➤ DenseNet (Densely Connected Convolutional Networks)

DenseNet, introduced by Huang et al. in 2017 [50], presents a novel convolutional architecture based on dense connectivity between layers. Unlike traditional CNNs, where each layer receives input only from the immediately preceding layer, DenseNet connects each layer to all previous layers. Specifically, the output of the l^{th} layer is a function of all preceding feature maps:

$$x_l = H_l([x_0, x_1, \dots, x_{l-1}])$$

where $[x_0, x_1, \ldots, x_{l-1}]$ denotes the concatenation of feature maps from layers 0 to $l - 1$.

This dense connectivity pattern promotes:

- Strong feature reuse, reducing the need to relearn redundant patterns.
- Efficient parameter usage, leading to a more compact model.
- Improved gradient flow, enabling the training of deeper networks without degradation.

Figure 15 present DenseNet architecture showing inter-layer dense connections.

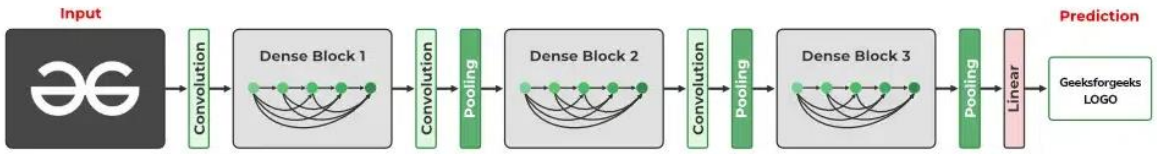


Figure 15: *Architecture of DenseNet [51]*

In this study, we employed the DenseNet-121 model, a moderate-depth variant comprising 121 layers organized into dense blocks separated by transition layers. DenseNet-121 offers a good balance between depth, computational cost, and generalization capability particularly valuable when working with limited datasets.

Advantages of DenseNet-121 in this context include:

- Efficient feature reuse, which is crucial for capturing fine-grained skin lesion patterns.
- Stable training, due to smooth gradient propagation.
- Strong generalization, minimizing overfitting on relatively small datasets.

Figure16 show the DenseNet-121 architecture overview.

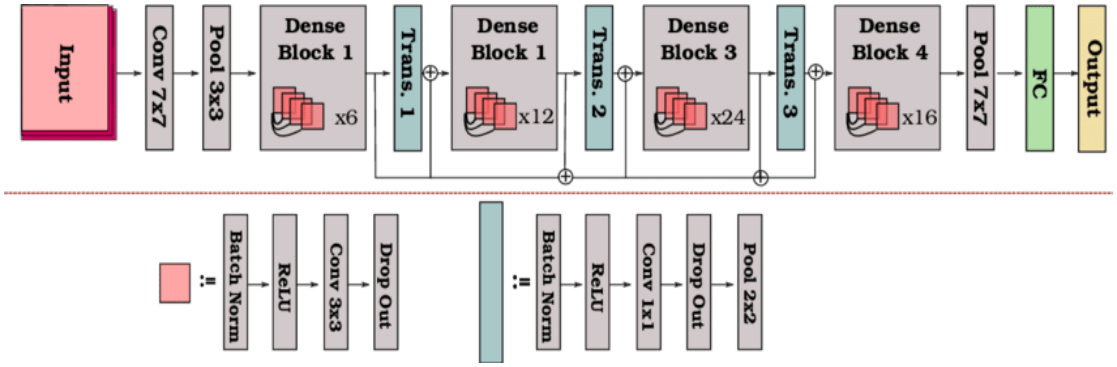


Figure 16: *DenseNet-121 architecture [52]*

However, the main drawback of DenseNet is its increased memory usage, resulting from the concatenation of multiple feature maps, which becomes significant as the network depth increases.

➤ Xception (Extreme Inception)

Xception, proposed by François Chollet in 2017 [53], is a deep convolutional neural network that builds upon the Inception architecture by extending it to an extreme. The name **Xception** stands for Extreme Inception, reflecting its design philosophy of replacing Inception modules with depthwise separable convolutions a more efficient and conceptually cleaner alternative.

This operation breaks a standard convolution into two sequential steps:

1. Depthwise convolution applies a single filter per input channel.
2. Pointwise convolution (1×1) combines the outputs across channels.

This separation significantly reduces the number of parameters and computational cost, while often maintaining or even improving classification performance [53]. Figure17 present Xception architecture

In our study, Xception was evaluated due to its:

- High efficiency, surpassing InceptionV3 despite having a comparable number of layers.
- Fully convolutional design, free of the complexity of traditional Inception modules.
- Strong capability in capturing subtle texture variations, essential for identifying complex skin disorders in dogs.

Overall, Xception stands out as a lightweight yet powerful architecture, well-suited for medical image classification tasks where computational resources and dataset size may be limited.

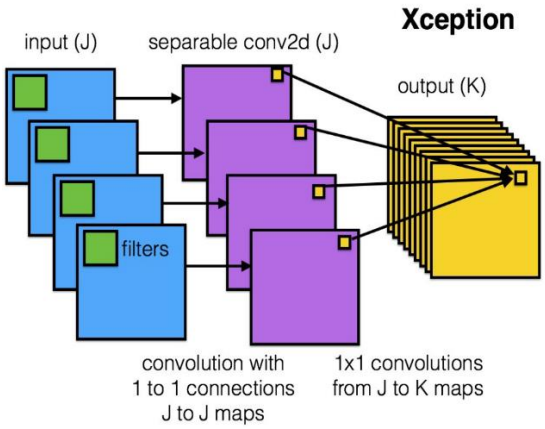


Figure 17: *Xception (Extreme Inception) architecture [54]*

➤ EfficientNet

EfficientNet, introduced by Tan and Le in 2019 [55], represents a significant advancement in model design through its use of compound scaling. Unlike conventional approaches that scale only one dimension of a network depth, width, or input resolution EfficientNet uniformly scales all three dimensions using a set of fixed scaling coefficients. This strategy results in a highly optimized trade-off between accuracy and efficiency. Figure 18 depict the EfficientNet architecture.

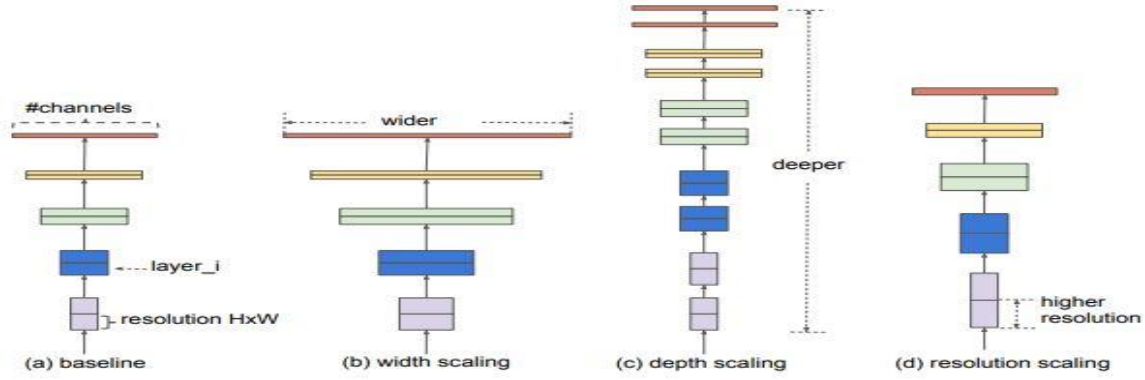


Figure 18: *EfficientNet architecture [56]*

EfficientNet is available in multiple variants (B0 to B7), with each successive model offering increased accuracy and computational requirements. In this study, we evaluated the following variants:

- **EfficientNetB0**:

  The baseline model of the EfficientNet family, offering a compact and computationally efficient architecture. It is particularly well-suited for environments with limited hardware resources, while still maintaining competitive performance. Figure19 show EfficientNet-B0.

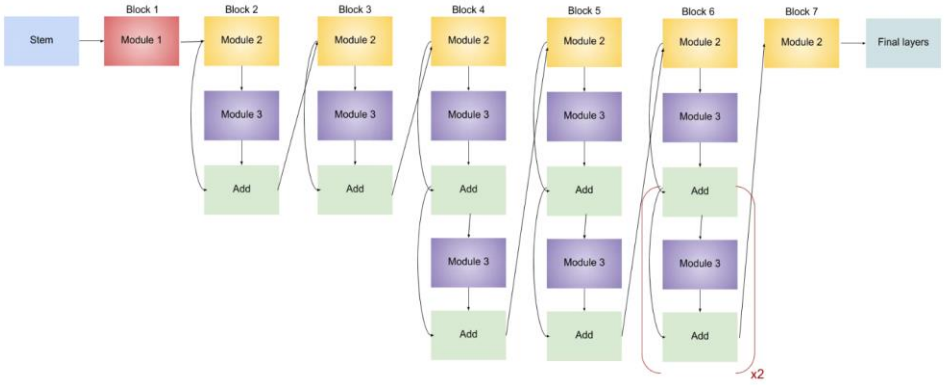


Figure 19: *Architecture of EfficientNet-B0 [57]*

- **EfficientNetB3**:

  Provides a balanced compromise between speed and accuracy, making it an excellent candidate for real-world deployment scenarios where both inference time and prediction quality are critical. Figure20 illustrate EfficientNet-B3.

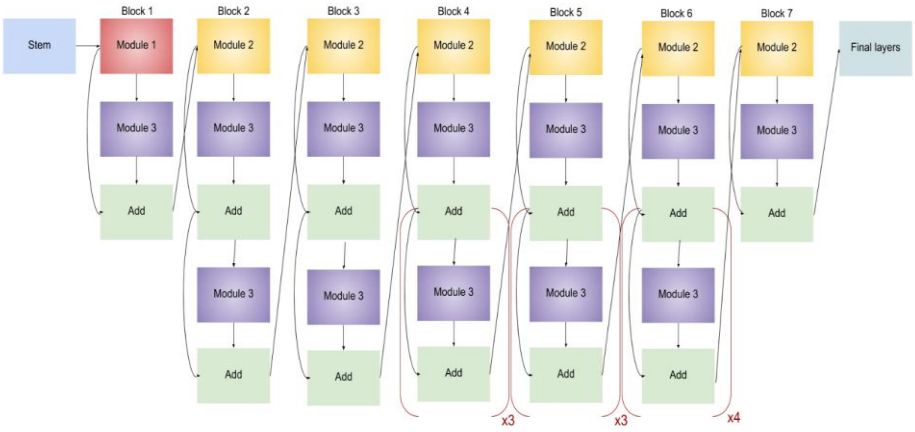


Figure 20: *Architecture of EfficientNet-B3 [56]*

- **EfficientNetB7**:

  The largest and most powerful version in the series, designed for high-precision tasks. It offers superior accuracy at the cost of increased computational demands. Figure21 show Architecture of EfficientNet-B7

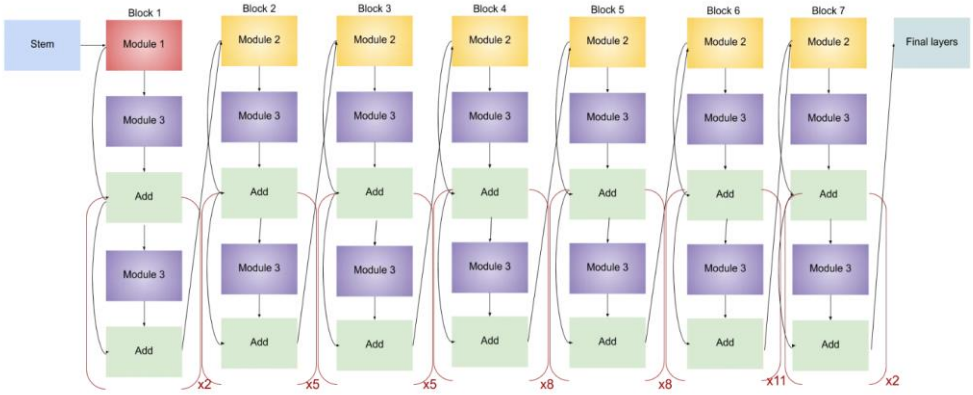


Figure 21 : *Architecture of EfficientNet-B7 [56]*

Key strengths of EfficientNet include:

- Outstanding parameter efficiency, enabling high performance with fewer trainable weights,
- Superior accuracy on small and large datasets, thanks to its optimized scaling approach,
- Excellent generalization, even for images containing subtle or fine-grained details, such as skin lesions.

➤ MobileNet Family

The MobileNet family of models is specifically designed for lightweight, fast execution in resource-constrained environments, such as mobile phones, IoT devices, and embedded systems. MobileNets achieve this efficiency primarily through the use of depthwise separable convolutions, which factorize standard convolutions into two simpler operations: depthwise and pointwise convolutions. This drastically reduces the number of parameters and computational load.

• **MobileNetV2**, proposed by Sandler et al. in 2018 **[57],** improves upon its predecessor by introducing:

- Inverted residual blocks, which allow shortcut connections between thin bottleneck layers,
- Linear bottlenecks, which prevent information loss after non-linear activations.

These enhancements allow the network to preserve representational power while remaining compact and efficient. Figure22 show Architecture of MobileNetV2

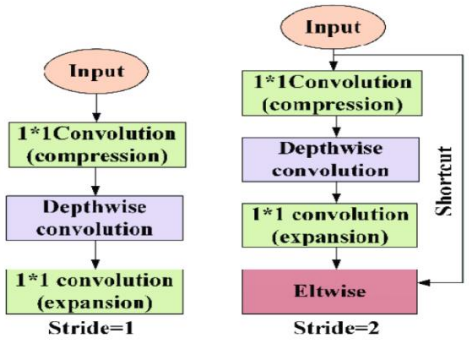


Figure 22: *MobileNetV2 Architecture [58]*

• **NASNetMobile**, developed by Zoph and Le in 2018 **[59]**, is a lightweight version of the NASNet architecture, which was discovered using Neural Architecture Search (NAS). NASNetMobile is designed by automatically searching for the optimal neural structure, producing a compact yet powerful model suited for mobile deployment.

Key advantages of MobileNet-based models include:

- Minimal memory and computational footprint, ideal for real-time applications,
- Good accuracy-efficiency trade-off, especially in mobile and edge computing scenarios,
- Robust performance, even when trained on relatively small datasets.

5.3. Selected Models

To evaluate the effectiveness of different deep learning approaches for classifying skin diseases in dogs, we selected a diverse set of pre-trained Convolutional Neural Network (CNN) architectures, all originally trained on the ImageNet dataset. These models are known for their strong generalization abilities and capacity to extract robust visual features across a wide range of image types.

The selected models encompass a variety of architectural paradigms, from lightweight designs optimized for mobile and embedded systems to deeper networks capable of learning complex hierarchical representations:

- **DenseNet121:** A densely connected network that promotes feature reuse and efficient gradient flow, particularly effective on complex textures.
- **InceptionV3:** An architecture that captures multi-scale features using parallel convolutions of varying kernel sizes, ideal for images with diverse lesion patterns.
- **Xception:** A depthwise separable convolution-based model that offers improved computational efficiency and performance over traditional Inception modules.
- **EfficientNet** (Variants **B0**, **B3**, and **B7):** These models scale network dimensions (depth, width, and resolution) in a balanced way using compound scaling, achieving a strong trade-off between performance and efficiency.
- **ResNet** (Variants **ResNet50** and **ResNet101):** Deep residual networks using identity skip connections to enable the training of very deep models without degradation in performance.
- **MobileNetV2:** A lightweight architecture designed for low-power devices, utilizing depthwise separable convolutions and inverted residuals.
- **NASNetMobile:** A mobile-optimized version of NASNet, generated through Neural Architecture Search to maximize accuracy under computational constraints.
- **VGG** (Variants **VGG16** and **VGG19):** Classical deep CNN architectures with uniform convolutional layers followed by fully connected layers, included for baseline comparison.

These models were chosen to ensure a comprehensive performance benchmark under varying computational budgets and image complexity levels. Their diverse design philosophies provide a robust basis for understanding which architectures are best suited for the classification of **canine dermatological conditions** using transfer learning.

5.4. Training Strategy of the Selected Pre-trained Models

To leverage the representational power of deep learning while minimizing the need for large labeled datasets, this study employs transfer learning using a set of pre-trained CNN models. Each model retains its convolutional base (include_top=False), effectively removing the original classification head designed for ImageNet. A custom classification head was appended to adapt the models to the specific task of multi-class classification of canine skin diseases (4 classes).

The custom classification head appended to each pre-trained base consists of the following components:

- Batch Normalization Layer: Stabilizes the learning process by normalizing the inputs to subsequent layers.

- Global Average Pooling Layer (GlobalAveragePooling2D): Reduces the spatial dimensions of the feature maps, resulting in a compact and informative representation.
- Three Fully Connected (Dense) Layers: Each layer uses ReLU activation and incorporates both L1 and L2 regularization to prevent overfitting.
- Batch Normalization and Dropout Layers: Placed after each dense layer to further enhance generalization and reduce the risk of overfitting.
- Output Layer: A dense layer with softmax activation to perform multi-class classification across four diagnostic categories.

5.4.1 Training Parameters

Each model is compiled and trained using the following hyperparameters and strategies:

- Optimizer: *Adam* chosen for its adaptive learning rate and fast convergence properties.
- Loss Function: *Categorical Crossentropy* suitable for multi-class classification tasks.
- Evaluation Metric: *Accuracy* monitored on both training and validation sets.
- Class Weights: Computed dynamically to mitigate class imbalance during training.
- Initial Learning Rate: 0.001 automatically reduced using a learning rate scheduler based on validation performance.
- Batch Size: 32 images per iteration.
- Number of Epochs: Up to 150 with early stopping enabled to terminate training when overfitting is detected.
- Early stopping: Patience=20 (monitoring val_loss)

5.4.2 Training and Evaluation Protocol

The CNN models are trained using an iterative procedure across multiple epochs, with performance closely monitored throughout:

1. **Training:** The model learns from the training dataset using mini-batch gradient descent.
2. **Validation**: After each epoch, performance is evaluated on the validation set to assess generalization.
3. **EarlyStopping**: If validation accuracy does not improve for 15 consecutive epochs, training is halted to prevent overfitting.
4. **ReduceLROnPlateau**: If no improvement is observed for 7 epochs, the learning rate is automatically reduced to fine-tune training dynamics.

6. Evaluation Results

6.1. Evaluation Metrics

To rigorously assess the classification performance of the deep learning models employed in this study, the following standard evaluation metrics were used:

- **Accuracy**: Represents the overall proportion of correctly classified samples across all classes.

$$\text{Accuracy} = \frac{TP + TN}{TP + TN + FP + FN}$$

Where:
TP: True Positives
TN: True Negatives
FP: False Positives
FN: False Negatives

- **Area Under the ROC Curve (AUC)**: Reflects the model's ability to distinguish between different classes. Values closer to 1 indicate superior discriminative performance. It is calculated as the area under the Receiver Operating Characteristic (ROC) curve:

$$\text{AUC} = \int_0^1 TPR(FPR)\ dFPR$$

Where:
TPR: True Positive Rate
FPR: False Positive Rate

- **Matthews Correlation Coefficient (MCC)**: A robust metric for imbalanced datasets, MCC ranges from -1 (total disagreement) to 1 (perfect prediction). The MCC is a balanced measure, especially valuable for imbalanced datasets:

$$\text{MCC} = \frac{(TP \cdot TN) - (FP \cdot FN)}{\sqrt{(TP + FP)(TP + FN)(TN + FP)(TN + FN)}}$$

It returns a value between -1 and 1:
+1: Perfect prediction
0: Random prediction
-1: Total disagreement between prediction and actual

- **F1-Score**: The harmonic mean of precision and recall, particularly valuable when dealing with class imbalance, defined as:

$$\text{F1-Score} = 2 \cdot \frac{\text{Precision} \cdot \text{Recall}}{\text{Precision} + \text{Recall}}$$

This metric is particularly useful in cases of class imbalance.

6.2 Performance of CNN Models on original Multispectral Images

Table 5 provides a comprehensive evaluation of various Convolutional Neural Network (CNN) architectures applied to the classification of animal skin diseases using multispectral images. Each model was assessed using multiple performance metrics, including accuracy, Area Under the Curve (AUC), Matthews Correlation Coefficient (MCC), F1-score, and the corresponding confusion matrix. These metrics offer a detailed view of each model's classification capability, robustness, and generalization across the four target classes. The results highlight the effectiveness of deep learning, particularly when combined with transfer learning, in addressing complex multiclass image classification tasks in the medical domain.

Table 4 . Performance of different CNN models on multispectral images.

Model	**Accuracy** (%)	**AUC** (%)	**MCC** (%)	**F1-score** (%)	**Confusion Matrix**
NASNetMobile	43.6	59.0	12.1	21.8	[[2,0,0,17], [4,1,2,13], [1,0,0,15], [0,0,1,38]]
VGG19	38.3	54.4	1.1	18.9	[[0,0,2,17], [0,0,3,17], [0,0,3,13], [0,0,6,33]]
MobileNetV2	35.1	52.3	9.7	21.6	[[0,11,0,8], [0,17,0,3], [0,5,0,11], [0,23,0,16]]
MobileNet	**92.6**	**99.6**	**89.6**	**91.0**	[[17,1,0,1], [0,19,0,1], [3,0,12,1], [0,0,0,39]]
VGG16	25.5	60.4	11.9	18.7	[[12,0,7,0], [7,0,13,0], [4,0,12,0], [19,0,20,0]]
ResNet50V2	84.0	93.6	77.6	83.2	[[15,1,1,2], [1,18,0,1], [1,0,12,3], [1,3,1,34]]
EfficientNetB3	**92.6**	**99.7**	**89.7**	**92.1**	[[18,0,0,1], [2,16,0,2], [1,0,15,0], [1,0,0,38]]
ResNet101	33.0	69.3	28.7	29.8	[[18,1,0,0], [8,12,0,0], [15,0,1,0], [38,1,0,0]]
EfficientNetB0	64.9	89.1	50.0	64.2	[[11,2,0,6], [0,15,1,4], [0,1,8,7], [7,2,3,27]]
DenseNet121	**87.2**	**97.1**	**82.1**	**86.0**	[[17,2,0,0], [0,17,1,2], [2,0,12,2], [3,0,0,36]]
InceptionV3	83.0	94.2	76.4	81.5	[[17,0,0,2], [1,19,0,0], [1,0,8,7], [5,0,0,34]]
Xception	**95.7**	**99.9**	**94.1**	**95.4**	[[18,1,0,0], [0,20,0,0], [1,0,15,0], [2,0,0,37]]

The results demonstrate that deep learning models, particularly those leveraging transfer learning, achieved excellent performance on the classification of animal skin diseases using multispectral imagery. Notably, the models Xception, EfficientNetB3, DenseNet121, InceptionV3, ResNet50V2, and EfficientNetB0 surpassed 80% accuracy, and exhibited high AUC, MCC, and F1-score values some approaching perfection (i.e., near 1.000).

These models also showed consistent generalization across the four-class problem, as evidenced by their well-distributed confusion matrices with minimal misclassification.

- Xception achieved the highest accuracy (95.7%) and F1-score (95.4%), confirming its strong representational power and robustness.
- EfficientNetB3 closely followed, with 92.6% accuracy and 92.1% F1-score, indicating both high precision and recall.
- DenseNet121 also performed well, achieving 87.2% accuracy with excellent class balance a crucial advantage in medical applications where false negatives can be harmful.
- MobileNet, although lightweight and optimized for resource-constrained environments, still delivered 92.6% accuracy, making it suitable for mobile deployment in rural or low-resource settings.

In contrast, older or shallower models such as VGG16, VGG19, and ResNet101 struggled, with accuracy ranging from 25% to 38% and very low F1-scores. These models failed to effectively capture the complex features inherent in multispectral images, as seen in their skewed confusion matrices and class biases.

This **Figure 23** highlights the superiority of advanced CNN models when applied to multispectral data. The integration of enriched spectral information significantly enhances the discriminatory power of deep learning models. In particular, Xception, EfficientNetB3, DenseNet121, and ResNet50V2 consistently achieve high scores across all performance metrics, confirming their robustness and reliability in complex classification tasks. These models are especially well-suited for deployment in real-world veterinary diagnostic systems, including in rural or resource-constrained environments, where accurate and efficient skin disease detection in animals is critical.

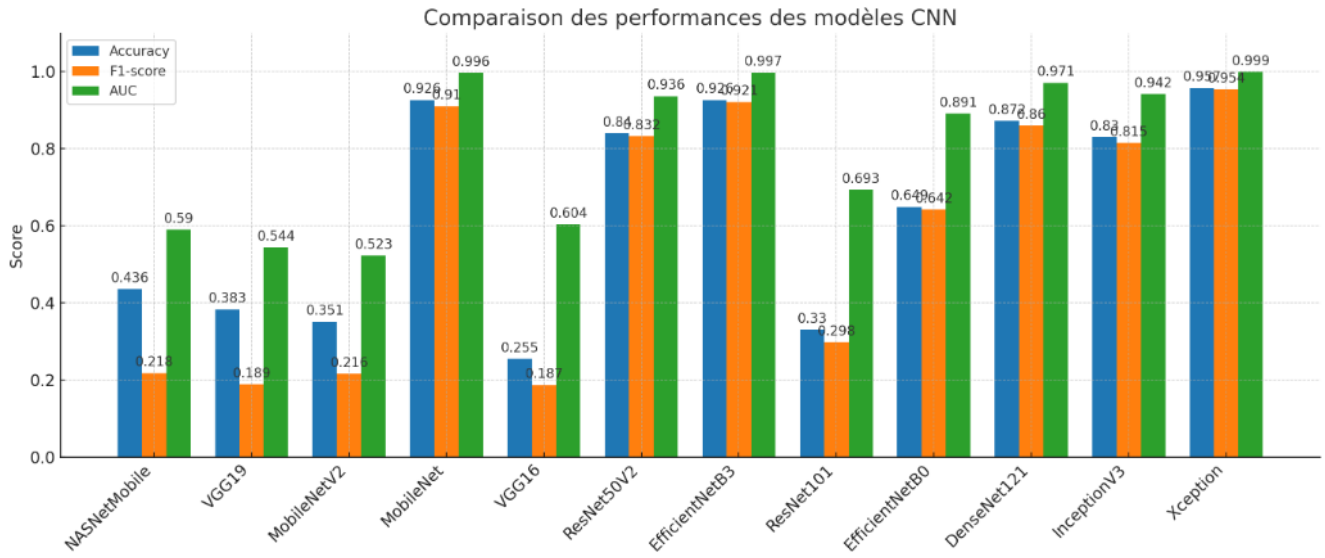


Figure 23: *Bar chart comparing the performance of various CNN models on multispectral images in terms of Accuracy, F1-score, and AUC.*

In conclusion, the analysis of multispectral images clearly demonstrates that incorporating enriched spectral information, in conjunction with advanced CNN architectures and carefully optimized hyperparameters, significantly enhances classification performance. Models such as Xception, EfficientNetB3, DenseNet121, and ResNet50V2 consistently deliver outstanding results, making them strong candidates for the development of intelligent veterinary diagnostic support systems. Their robustness and efficiency make them particularly suitable for deployment in real-world settings, especially in rural or resource-limited areas, where access to expert medical evaluation may be constrained.

6.3. Performance of the Xception Model Using Data Augmentation

To enhance the model's robustness and reduce overfitting caused by limited training data, a data augmentation strategy was implemented during the training phase. This approach involves generating new training samples from the original dataset by applying a sequence of carefully chosen transformations that simulate natural variations in the data.

In this study, the following augmentation techniques were applied to each original image:

- **Random Horizontal Flip**: Simulates left-right symmetry variations by randomly flipping images along the vertical axis.
- **Random Vertical Flip**: Introduces additional variability by flipping images top to bottom.
- **Random Rotation (90°, 180°, 270°)**: Uses random 90-degree rotations to increase orientation diversity.

- **Random Translation**: Introduces slight shifts in image content by applying random horizontal and vertical displacements within a range of -10 to +10 pixels.
- **Padding and Cropping**: Ensures the image remains at a fixed size after transformation by padding it to a larger bounding box (148×148 pixels) followed by cropping it back to the original size (128×128 pixels).

These transformations were applied using TensorFlow's image processing functions, and multiple augmented versions were generated per image to significantly expand the diversity of the training dataset. As illustrated in **Figure 24**, the introduction of this data augmentation pipeline led to notable improvements in the training behavior and generalization performance of the Xception model:

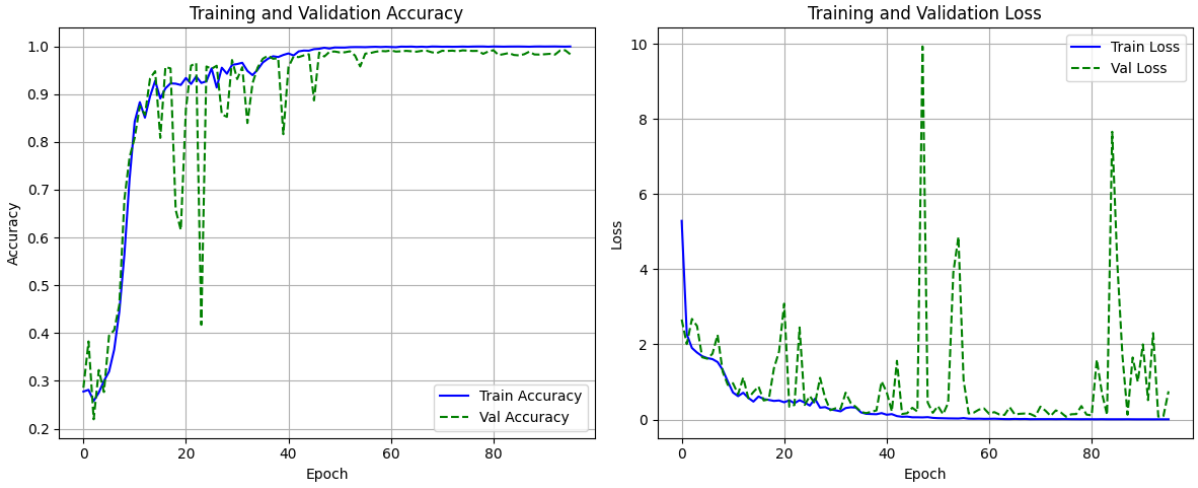


Figure 24: *Training and validation accuracy and loss curves of the Xception model after applying data augmentation.*

Key improvements observed:

- **Accuracy:** Training and validation accuracy curves became more stable and aligned, converging around 98.9%, indicating strong generalization with minimal overfitting.
- **Loss:** Validation loss dropped below 0.2 and remained low throughout training, compared to the erratic and elevated loss levels seen before augmentation.
- **Stability:** The reduced gap between training and validation curves confirms that the model benefited from the added data variability and is now more robust when applied to unseen data.

In conclusion, the use of tailored data augmentation techniques proved highly effective in enhancing the performance of the Xception model, making it better suited for real-world deployment in veterinary diagnostic support systems, especially in scenarios where data availability is limited.

6.3.1 Performance Comparison Before and After Applying Data Augmentation

To evaluate the impact of the data augmentation strategy, a direct comparison was conducted between the performance of the Xception model trained without augmentation and with augmentation. The comparison is summarized in the table below:

Table 5 . Comparative Performance of the Xception Model with and without Data Augmentation

Metric	Without Augmentation	With Augmentation
Accuracy	95.7	98.9
F1-score	95.4	98.7
MCC	94.1	98.4
AUC	99.9	99.7

The results indicate that applying data augmentation led to significant improvements across all performance metrics. Notably, accuracy increased by over 3 percentage points, and the F1-score and Matthews Correlation Coefficient (MCC) also rose substantially. These enhancements reflect the model's improved capacity to accurately and consistently classify samples from all classes, especially those that may have been underrepresented in the original dataset.

A comparison of the confusion matrices before and after augmentation **(Figure 25)** further illustrates this improvement:

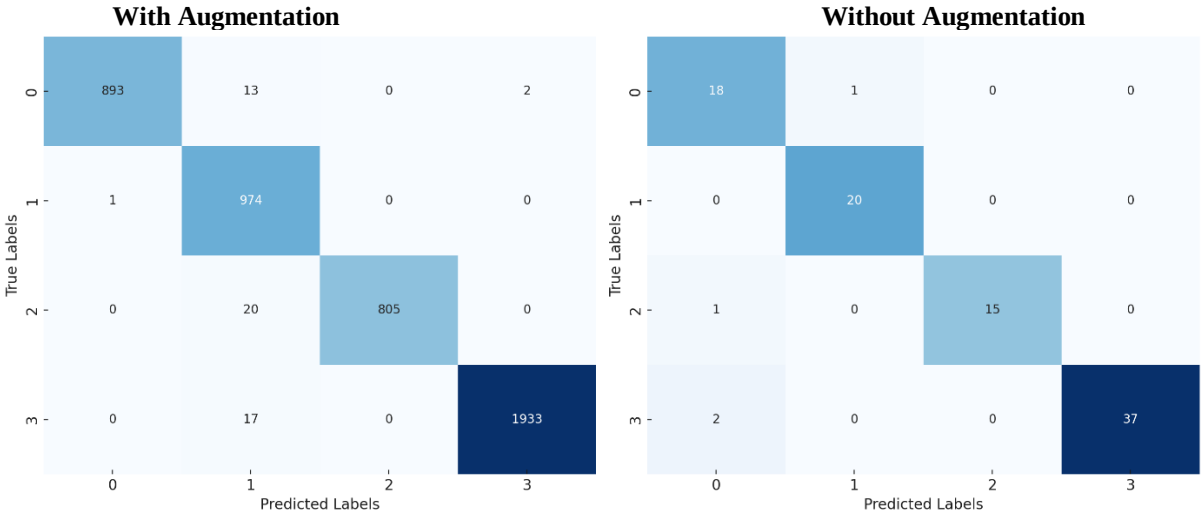


Figure 25: *Confusion Matrices of the Xception Model Before and After Data Augmentation.*

The confusion matrix after augmentation reveals a dramatic reduction in classification errors. For example:

- In **Class 3(**Bacterial_dermatosis**)**, 1933 out of 1950 samples were correctly classified.
- In **Class 0(**Fungal_infections**)**, only 2 misclassifications occurred out of 908 samples.

These results underscore the augmented model's greater robustness and reliability in handling diverse and visually similar input data.

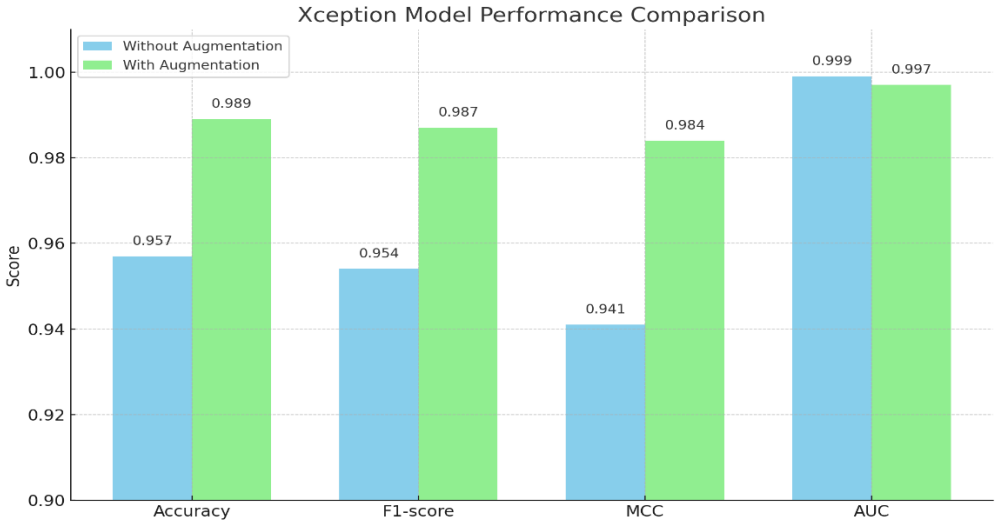


Figure 26: *Performance Comparison of the Xception Model With and Without Data Augmentation.*

As shown in **Figure 26**, the performance of the Xception model significantly improves when data augmentation techniques are applied. The model demonstrates higher scores across all evaluation metrics Accuracy, F1-score, MCC, and AUC when trained with augmented data. This confirms that data augmentation enhances the model's generalization ability and reduces classification errors, particularly those caused by class imbalance or visual similarity among categories. Such improvements are especially valuable in veterinary image classification, where datasets often lack sufficient representation for all disease conditions. Based on these findings, incorporating data augmentation should be considered a critical step in the development pipeline for deep learning-based image classification models in similar applications.

7. Comparative Analyses

To objectively assess the performance of our proposed model, we compared our results with those reported in the reference study by **Hwang et al. (2022) [19]**, which is considered a foundational work in the classification of canine skin diseases using deep learning and multispectral imaging. The following table highlights comparison classification techniques, dataset typesand key performance metrics.

Table 6 . Comparative summary of methodologies and results

Author	Deep CNN Model	Dataset Used	Results
Hwang et al. (2022) [19]	Consensus model of Conventional CNNs (DenseNet, InceptionNet)	Multispectral & Normal Images	Accuracy: 89%, MCC: 76%, AUC: 87–89%, F1-score: Not reported
Our Study (2025)	Pre-trained CNNs (Xception) + Data Augmentation	Multispectral dataset (canine images)	Accuracy: 98.9%, F1-score: 98.7%, AUC: 99.7%, MCC: 98.4%

The comparative evaluation between our multispectral CNN-based classification pipeline and the work of Hwang et al. (2022) **[19]** reveals critical differences in methodology, architecture choice, and predictive performance for dog skin disease diagnosis. While both approaches leverage multispectral imaging for dermatological analysis, the implementation strategies yield substantially different outcomes.

Our deep learning framework demonstrates that the integration of transfer learning with modern architectures such as **Xception,** , combined with advanced data augmentation and class wheight techniques, leads to **superior generalization and robustness**, particularly in multi-class classification contexts. The use of pretrained models on **ImageNet** enables efficient feature reuse, improving both convergence speed and discriminative power across disease categories.

In contrast, the study by Hwang et al. utilizes classical CNN architectures trained from scratch without pre-initialized weights, resulting in **limited performance gains**, especially in validation phases. Their consensus model approach, while effective in boosting metrics over single-source models, still exhibits **lower accuracy (max 89%) and MCC (max 76%)** when compared to our unified pipeline, which achieves **accuracy of 98.9% and MCC of 98.4%** with a single well-optimized model.

Moreover, Hwang's binary classification framework, though methodologically simpler, introduces scalability limitations when handling complex, real-world multi-disease scenarios. In contrast, our pipeline's **multi-class structure** proves more practical and reflective of real diagnostic applications. Additionally, performance metrics such as **F1-score (98.7%) and AUC (99.7%)** in our study confirm the classifier's ability to maintain balance between sensitivity and specificity, even in imbalanced datasets.

Overall, our methodology provides a **more accurate, extensible, and deployment-ready solution** for veterinary skin disease diagnosis using multispectral imaging. The combination of transfer learning, robust augmentation, and efficient architecture selection allows our model to outperform prior benchmarks and sets a foundation for future integration in real-time or mobile diagnostic tools.

8. Limitations and Future Perspectives

8.1. Limitations

Despite the promising results achieved in this study, several limitations should be acknowledged. First, the size and diversity of the dataset were limited, which may reduce the model's ability to generalize across various animal species and environmental conditions. Second, the model's performance heavily depends on the accuracy and reliability of the annotated data, which may contain errors or biases due to manual labeling or expert variability. Third, the computational resources required for training deep learning models were substantial, limiting the feasibility of deploying the system in farms or regions with limited infrastructure. Finally, the inherently "black-box" nature of deep learning models poses challenges for interpretability, which is critical in veterinary applications where transparency in diagnosis is essential.

8.2. Future Perspectives

To enhance the system's performance and practical applicability, it is necessary to expand the dataset by including a larger number of samples and a wider range of animal species while accounting for diverse environmental conditions. Incorporating multimodal data sources, such as multispectral imaging or clinical data, could further improve classification accuracy. Additionally, developing more efficient and lightweight models would facilitate deployment

on mobile devices used in field conditions. Improving model interpretability through explainable AI techniques is also essential to build trust among veterinarians and farmers. Lastly, future work should focus on validating the models in real-world environments and adopting continuous learning strategies to update the models with new data, ensuring sustained performance over time.

9. Conclusion

This chapter presented a comprehensive evaluation of various deep learning models for the classification of animal skin diseases using multispectral images. The results demonstrated that state-of-the-art architectures, such as Xception and EfficientNetB3, achieved superior performance, exhibiting high classification accuracy and strong generalization capabilities. In contrast, older or shallower models, including VGG16 and VGG19, struggled to capture the complex features in multispectral data, resulting in significantly lower accuracy and higher misclassification rates.

The application of data augmentation techniques proved particularly beneficial especially for the Xception model by increasing model robustness, reducing overfitting, and enhancing generalization across diverse classes. These findings underscore the critical role of both advanced CNN architectures and training strategies in building effective and scalable veterinary diagnostic systems.

Moreover, the integration of multispectral imaging, which captures rich spectral information beyond standard

General Conclusion

General Conclusion

This research emphasized the crucial need for automated diagnostic tools for animal skin diseases, especially in rural areas with limited veterinary access. By integrating multispectral imaging with deep learning techniques, we developed an effective system capable of accurately classifying skin conditions in dogs.

The proposed approach leveraged advanced CNN architectures such as Xception, EfficientNet, and DenseNet121, … etc , trained on a curated dataset of multispectral images. Data augmentation and class balancing techniques contributed to improved model performance. Among the models, Xception achieved outstanding results, with 98.9% accuracy and an AUC of 99.7%, demonstrating the strong potential of our method.

Beyond its academic contribution, this system provides a practical and accessible diagnostic aid, particularly valuable in underserved regions. Future work could involve expanding the dataset to cover more diseases and species, implementing real-time mobile solutions, and exploring hybrid and interpretable models to increase trust and usability among veterinary professionals.

Bibliography

[01] BENEDETTI JULIA. (2024, January). *Évaluation du patient dermatologique* (Vol. 2024). Vol. 2024. Retrieved from https://www.msdmanuals.com/fr/professional/troubles-dermatologiques/prise-en-charge-du-patient-atteint-de-troubles-dermatologiques/évaluationdu-patient-dermatologique

[**02**] (N.d.). Retrieved 26 May 2025, from https://dermnetnz.org/topics/the-structure-of-normal-skin(DermNet®)

[03] Fraperie, P. (2016, September 2). Anatomie fonctionnelle de la peau -. Retrieved 26 May 2025, from https://microbiologiemedicale.fr/peau-anatomie/

[04] Bessaguet, F., Seuve, É., & Desmoulière, A. (2022). La peau. *Actualités Pharmaceutiques*, *61*(615), 57–61. doi:10.1016/j.actpha.2022.02.014

[05] André. (2021, July 6). Schéma de la peau complet et avec légende. Retrieved 26 May 2025, from Information hospitalière : Lexique et actualité du milieu médical website: https://www.informationhospitaliere.com/schema-de-la-peau-complet-et-avec-legende

[06] Tortora, G. J., & Derrickson, B. H. (2017). *Principles of Anatomy and Physiology*. Hoboken, NJ, USA: Wiley.

[**07]** "Hypoderme : définition, rôle, schéma," *Journal des Femmes Santé*, 20 juin 2022

[08] Elias, P. M. (2005). Stratum corneum defensive functions: an integrated view. *The Journal of Investigative Dermatology*, *125*(2), 183–200. doi:10.1111/j.0022-202X.2005.23668.x

[09] Mackey, H. O. (1968). *Physiology and Pathology of the Skin* (pp. 6–8). Palgrave, London. https://doi.org/10.1007/978-1-349-15275-9_2

[10] Marks, J. G., & Miller, J. J. (2013). *Structure and Function of the Skin* (pp. 2–10). W.B. Saunders. https://doi.org/10.1016/B978-1-4557-2875-6.00002-9

[11] Rodrigues, M., Ezzedine, K., Hamzavi, I., Pandya, A. G., & Harris, J. E. (2017). New discoveries in the pathogenesis and classification of vitiligo. *Journal of the American Academy of Dermatology*, *77*(1), 1–13. doi:10.1016/j.jaad.2016.10.048

[12] Olivry, T. (2018). Auto-immune skin diseases in animals: time to reclassify and review after 40 years. *BMC Veterinary Research, 14*(1). doi:10.1186/s12917-018-1477-1

[13] Johns, N. E., Hay, R. J., Wulf, S., & Naghavi, M. (2013). A systematic analysis of the global burden of skin disease: lesions learned. *The Lancet*, *381*. https://doi.org/10.1016/S0140-6736(13)61321-5

[14]Alautaish, H. H., Naji, H. A., & Saud, Z. A. H. (2024). Clinical study of common bacterial, fungal and parasitic skin diseases in cats. *Advances in Life Sciences*. https://doi.org/10.62940/als.v11i3.1873

[15] Elitok, B., & Kislalioglu, I. (2018). *Skin diseases: a review*. *1*(6), 269–270. https://doi.org/10.15406/MOJCRR.2018.01.00044

[16] Lloyd, D. H. (1993). *The Skin Microflora and Microbial Skin Disease: Viral skin disease in animals* (pp. 315–330). Cambridge University Press. https://doi.org/10.1017/CBO9780511527012.014

[17] Webster, S. B., & Uhler, D. M. (1986). Common skin conditions in humans and animals. *American Family Physician*, *33*(4), 177–182. https://pubmed.ncbi.nlm.nih.gov/2421568/

[18]Scott, D. W., Wolfe, M. J., Smith, C. A., & Lewis, R. M. (1980). The Comparative Pathology of Non-Viral Bullous Skin Diseases in Domestic Animals. *Veterinary Pathology*, *17*(3), 257–281. https://doi.org/10.1177/030098588001700301

[19]Zhang, J. Y. (2017). *Animal Models of Skin Disorders* (pp. 357–375). Academic Press. https://doi.org/10.1016/B978-0-12-809468-6.00015-2

[20] Shinde, P. P., & Shah, S. (2018). A Review of Machine Learning and Deep Learning Applications. *2018 Fourth International Conference on Computing Communication Control and Automation (ICCUBEA)*, 1–6. doi:10.1109/ICCUBEA.2018.8697857

[21] Goodfellow, I., Bengio, Y., & Courville, A. (2016). *Deep Learning*. MIT Press.

[22] Azevedo, B. F., Rocha, A. M. A. C., & Pereira, A. I. (2024). Hybrid approaches to optimization and machine learning methods: a systematic literature review. *Machine Learning*, *113*(7), 4055–4097. doi:10.1007/s10994-023-06467-x

[23] Kumar, A., Kumar, B., & Negi, H. S. (2023). Predicting Lumpy Skin Disease using Various Machine Learning Models. *2023 International Conference on Computational Intelligence and Sustainable Engineering Solutions (CISES)*, 412–416. doi:10.1109/CISES58720.2023.10183604

[24] Olaniyan, O. M., Adetunji, O. J., & Fasanya, A. M. (2023). Development of a model for the prediction of lumpy skin diseases using machine learning techniques. *ABUAD Journal of Engineering Research and Development*, *6*(2), 100–112. Retrieved from

[25] Wei, M., Wu, Q., Ji, H., Wang, J., Lyu, T., Liu, J., & Zhao, L. (2023). A Skin Disease Classification Model Based on DenseNet and ConvNeXt Fusion. *Electronics*, *12*(2), 438. https://doi.org/10.3390/electronics12020438

[26] Kritika Sujay Rao, P., Suresh Yelkar, O., & Narayan Pise, D. (2021). Skin Disease Detection using Machine Learning. *INTERNATIONAL JOURNAL OF ENGINEERING RESEARCH & TECHNOLOGY (IJERT) NTASU*, *2020*(03).

[27] Li, L.-F., Wang, X., Hu, W.-J., Xiong, N. N., Du, Y.-X., & Li, B.-S. (2020). Deep Learning in Skin Disease Image Recognition: A Review. *IEEE Access*, *8*, 208264–208280. doi:10.1109/ACCESS.2020.3037258

[28] Mujahid, M., Khurshaid, T., Safran, M., Alfarhood, S., & Ashraf, I. (2024). Prediction of lumpy skin disease virus using customized CBAM-DenseNet-attention model. *BMC Infectious Diseases*, *24*(1), 1181. doi:10.1186/s12879-024-10032-9.

[29] Hwang, S., Shin, H. K., Park, J. M., Kwon, B., & Kang, M.-G. (2022). Classification of dog skin diseases using deep learning with images captured from multispectral imaging device. *Molecular & Cellular Toxicology*, *18*(3), 299–309. doi:10.1007/s13273-022-00249-7.

[30] Senthilkumar, C., C, S., Vadivu, G., & Neethirajan, S. (2024). Early detection of lumpy Skin Disease in cattle using deep learning-A comparative analysis of pretrained models. *Veterinary Sciences*, *11*(10). doi:10.3390/vetsci11100510

[31] Bajwa, M. N., Muta, K., Malik, M. I., Siddiqui, S. A., Braun, S. A., Homey, B., Dengel, A., & Ahmed, S. (2020). Computer-Aided Diagnosis of Skin Diseases Using Deep Neural Networks. *Applied Sciences*, *10*(7), 2488. https://doi.org/10.3390/app10072488

[32] Sun, J., Yao, K., Huang, G., Zhang, C., Leach, M., Huang, K., & Yang, X. (2023). Machine Learning Methods in Skin Disease Recognition: A Systematic Review. *Processes*, *11*(4), 1003. https://doi.org/10.3390/pr11041003

[33] Rhaimi.Kh. K, Said.C.B. (2024). *Melanoma Skin Cancer Detected Based on Artificial Intelligence - Survey*. *36*, 29–30. doi:www.doi.org/10.62341/ISTJ

[34] Mahum, R., & Aladhadh, S. (2022). Skin Lesion Detection Using Hand-Crafted and DL-Based Features Fusion and LSTM. *Diagnostics*, *12*(12), 2974. https://doi.org/10.3390/diagnostics12122974

[35] Debelee, T. G. (2023). Skin Lesion Classification and Detection Using Machine Learning Techniques: A Systematic Review. *Diagnostics*, *13*(19), 3147. https://doi.org/10.3390/diagnostics13193147

[36] (n.d.-a). Retrieved 30 May 2025, from https://www.kaggle.com/search

[37] International Skin Imaging Collaboration. (2020). *SIIM-ISIC 2020 Challenge Dataset* [Data set]. doi:10.34970/2020-DS01

[38] Afshari Safavi, E. (2021). *Lumpy Skin disease dataset* [Data set]. doi:10.17632/7PYHBZB2N9.1

[39] Tschandl, P., Rosendahl, C., & Kittler, H. (2018). The HAM10000 dataset, a large collection of multi-source dermatoscopic images of common pigmented skin lesions. *Scientific Data*, *5*(1), 180161. doi:10.1038/sdata.2018.161

[40] Goel, S. (2020). *Dermnet* [Data set]. Retrieved from https://www.kaggle.com/datasets/shubhamgoel27/dermnet

[41] Hwang, S. (2022). *Classification of pet dog skin diseases using deep learning with images captured from multispectral imaging device* [Data set]. doi:10.17632/5DBHT54KW7.

[42] Fareez, M. M. M., Thangarajah, V., & Saabith, S. (11 2020). *POPULAR PYTHON LIBRARIES AND THEIR APPLICATION DOMAINS*.

[43] Comment, info, M.A, AlindGupta, & Follow. (2024, May 22). Getting started with Kaggle : A quick guide for beginners. GeeksforGeeks. https://www.geeksforgeeks.org/getting-started-with-kaggle-a-quick-guide-for-beginners/

[44] Manaswi, N. K. (n.d.). Understanding and Working with Keras. In *Deep Learning with*.

[45] Ragan-Kelley, B., Pérez, F., Granger, B., Bussonnier, M., Frederic, J., & Kelley, K. (n.d.). *Jupyter Notebooks - a publishing format for reproducible computational workflowsAuthorsThomas Kluyver*. Jessica Hamrick, Jason Grout, Sylvain Corlay, Paul Ivanov, Damián Avila, Safia Abdalla, Carol Willing.

[46] He, K., Zhang, X., Ren, S., & Sun, J. (2015a). Deep residual learning for image recognition. Retrieved from http://arxiv.org/abs/1512.03385

[47] He, K., Zhang, X., Ren, S., & Sun, J. (2016). Deep Residual Learning for Image Recognition. *2016 IEEE Conference on Computer Vision and Pattern Recognition (CVPR)*, 770–778. doi:10.1109/CVPR.2016.90

[48] Szegedy, C., Vanhoucke, V., Ioffe, S., Shlens, J., & Wojna, Z. (2016). Rethinking the Inception Architecture for Computer Vision. *2016 IEEE Conference on Computer Vision and Pattern Recognition (CVPR)*, 2818–2826. doi:10.1109/CVPR.2016.308

[49] Szegedy, C., Vanhoucke, V., Ioffe, S., Shlens, J., & Wojna, Z. (2015b). Rethinking the inception architecture for computer vision. doi:10.48550/ARXIV.1512.00567

[50] Huang, G., Liu, Z., Van Der Maaten, L., & Weinberger, K. Q. (2017). Densely Connected Convolutional Networks. *2017 IEEE Conference on Computer Vision and Pattern Recognition (CVPR)*, 2261–2269. doi:10.1109/CVPR.2017.243

[51] G. Huang, Z. Liu, L. Van Der Maaten, and K. Q. Weinberger, 'Densely Connected Convolutional Networks', in *2017 IEEE Conference on Computer Vision and Pattern Recognition (CVPR)*, 2017, pp. 2261–2269.

[52] Radwan, N. (2019). *Leveraging sparse and dense features for reliable state estimation in urban environments*. doi:10.6094/UNIFR/149856

[53] Chollet, F. (2017, July). Xception: Deep Learning with Depthwise Separable Convolutions. *2017 IEEE Conference on Computer Vision and Pattern Recognition (CVPR)*, 1800–1807. doi:10.1109/CVPR.2017.195

[54] *Xception architectural design*. coding. (n.d.). https://stephan-osterburg.gitbook.io/coding/coding/ml-dl/tensorfow/ch3-xception/xception-architectural-design

[55] M. Tan and Q. Le, "EfficientNet: Rethinking model scaling for convolutional neural networks," in *Proc. 36th Int. Conf. Mach. Learn. (ICML)*, Long Beach, CA, USA, 2019, vol. 97, pp. 6105–6114

[56] Imane, C. (2022, November 5). EfficientNet [model architecture]. Retrieved 26 May 2025, from OpenGenus IQ: Learn Algorithms, DL, System Design website: https://iq.opengenus.org/efficientnet/.

[57] Sandler, M., Howard, A., Zhu, M., Zhmoginov, A., & Chen, L.-C. (2018, June). MobileNetV2: Inverted Residuals and Linear Bottlenecks. *2018 IEEE/CVF Conference on Computer Vision and Pattern Recognition (CVPR)*, 4510–4520. doi:10.1109/CVPR.2018.00474

[58] Wang, Y., Yan, J., Sun, Q., Li, J., & Yang, Z. (2019). A MobileNets Convolutional Neural Network for GIS Partial Discharge Pattern Recognition in the Ubiquitous Power Internet of Things Context: Optimization, Comparison, and Application. *IEEE Access*, *7*, 150226–150236. doi:10.1109/ACCESS.2019.2946662

[59] Adedoja, A. O., Owolawi, P. A., & Mapayi, T. (2021). *Intelligent Mobile Plant Disease Diagnostic System Using NASNet-Mobile Deep Learning*. Retrieved from https://api.semanticscholar.org/CorpusID:252081398